scientific reports

Check for updates

OPEN

Lethality level casualty assessment method for earthquake landslide hazards based on the expansion effect of the mortality rate

Xia Chaoxu[1,2]✉, Qi Wenhua[1,2]✉, Li Huayue[1,2,3] & Nie Gaozhong[1,2]

Rapid assessment of earthquake disaster losses is crucial for effective emergency rescue operations, with post-earthquake geological hazards constituting a significant component. In this study, we conducted extensive field investigations of historical earthquakes in China, collecting mortality data categorized by cause of death. Through analysis of historical earthquake records, we determined the proportions of fatalities attributed to different causes, integrating seismic intensity data, population distribution information, to establish intensity-dependent mortality rates for earthquake-triggered landslides. We systematically compiled the spatial distribution patterns, occurrence frequency, and density characteristics of landslides induced by historical earthquakes through field surveys and literature analysis. By comparing these results with historical intensity-mortality relationships, we quantified the amplifying effect of secondary geological hazards on mortality rates. The results demonstrate that landslide hazards exhibit significant mortality amplification at intensities of VIII and above, with this amplification effect intensifying progressively with higher seismic intensities. Using these findings, we developed a lethality matrix for earthquake-triggered landslides by incorporating intensity-mortality relationships. Validation using historical earthquake cases shows that the calculated casualties error within ± 30% of actual recorded values across different regions and magnitudes. This study achieves two objectives (1) verifies the validity and regional applicability of the proposed matrix methodology for landslide casualty assessment, and (2) provides a scientific foundation for developing regionalized assessment matrices, thereby enhancing post-earthquake emergency response capabilities.

Keywords Secondary landslides, Mortality rate, Multiple relationships, Expanding effect, Lethality matrix

Earthquakes are sudden natural disasters that cause structural damage, casualties, economic losses, and a cascade of secondary hazards. Related research shows that when the magnitude is greater than 4.0, it will trigger geological disasters such as landslides and collapses[1,2]. When the magnitude is less than 5.0, the intensity is less than VI, secondary geological disasters rarely occur, with magnitudes ranging from 5.0 to 6.0 and intensities ranging from VI to VII. Earthquake secondary geological disasters generally occur, with a large number of magnitudes greater than 6.0 and intensities above VII. Secondary geological disasters are strong, not only large in number but also large in scale[3,4].

After an earthquake, the first concern is casualties. Since 1900, approximately 1% of destructive earthquakes have caused 93% of global deaths; secondary disasters have caused approximately 40% of economic losses and 17% of deaths[5–7]. Rapidly assessing casualties after an earthquake is the basis of all work, although a variety of earthquake casualty assessment methods already exist. However, since most of the current related evaluation methods consider only the damage of buildings, there are few casualty assessment methods for secondary earthquake landslides; therefore, how to carry out rapid assessments of causalities caused by secondary landslides is an important part of earthquake disaster research.

Different scholars have also carried out research on methods related to earthquake secondary landslides based on different research concepts, generally including two methods, the Newmark displacement model and

[1]Key Laboratory of Seismic and Volcanic Hazards, Earthquake Administration, Yard No.1, Hua Yan Li, Chaoyang District, Beijing 100029, China. [2]Institute of Geology, China Earthquake Administration, Yard No.1, Hua Yan Li, Chaoyang District, Beijing 100029, China. [3]China Earthquake Administration, No. 5, Nanheng Street, Sanlihe, Xicheng District, Beijing, China. ✉email: xiachaoxu@ies.ac.cn; qiwenhua@ies.ac.cn

its derived models[8–14] and correlation analysis methods based on landslide sensitivity[15–20]; however, most of the existing studies are based on postearthquake geological disaster databases to evaluate the probability of landslide occurrence[21–29], and the methods used are different, such as the methods of information acquisition analysis[30], logistic regression methods[31,32], analytic hierarchy process methods[33,34], fuzzy mathematics methods[35], artificial neural network methods[36], influence factor certainty coefficient methods[37].

Although related research has shown that earthquakes that cause landslides typically cause more fatalities (a cascading hazard) than earthquakes without landslides[38], a critical component of understanding landslide risk involves the assessment of landslide hazards, and multiple studies have attempted to provide a global estimation of this hazard[6,39]. Others have focused on the probability of landslide occurrence based on physical susceptibility factors[40–43]; however, the current situation is that little effort has focused on modeling the socioeconomic losses associated with landslides, relatively few methods, and currently none available to estimate the number of fatalities due to earthquake-induced landslides[44–48].

The basic idea of the evaluation method is based on the results of landslide probability, combined with population of exposure to construct the assessment method[49–57]. For example, Nowicki et al. established a multiple regression model based on the calculation results of landslide probability and population exposure index and carried out an order-of-magnitude estimate of the casualties data of earthquake-induced landslides[41,58,59]. Saeed et al. proposed a new method for estimating the probability of permanent displacement of mountain slopes using a Bayesian network and Newmark displacement probability modeling, which can be used to analyze the degree of losses and casualties caused by earthquakes[60]. Tonje et al. based on data from 66 historical landslide events that occurred in Norway and Sweden from 1848 to 2009 and estimated the death curve as a function of the number of people exposed to each landslide[61].

Although these studies have carried out the quantification and calculation of risk levels through the probability analysis of earthquake-induced landslides, there is still a lack of research on the assessment methods of casualties caused by earthquake secondary landslides. There is no necessary connection between the probability of landslide occurrence and the mortality rate because the probability of landslide occurrence is high, which does not necessarily mean that the corresponding mortality rate is also high; that is, if there is a landslide in an area, it cannot be directly assumed that death will be caused in the area, and there is a probabilistic relationship between earthquake-induced landslides and the mortality rate. This probability is actually directly related to factors such as the intensity, and the comprehensive level reflected by the geographical and geomorphological conditions of the secondary landslides, etc.; thus, establishing the relationships among the intensity, comprehensive level and mortality rate is the key to assessing earthquake secondary landslide casualties.

It is necessary to propose a quantitative estimation model for causalities to mitigate the risk of earthquake-induced landslides. In this paper, we perform a correlation analysis of the mortality rate and the landslide data (landslide density) of different intensities and establish a model based on intensity, secondary landslides and mortality rate, all of which are specifically used to disaggregate the direct effects of ground shaking from those associated with secondary landslides. Based on this, we constructed a lethality matrix for earthquake secondary landslides to achieve rapid assessment of casualties.

Data and methods

Data

At present, several international databases related to damaging earthquakes have been developed, such as the Emergency Disasters Database (EM-DAT), the Natural Catastrophe Loss Database (NatCatSERVICE), the Global Disaster Identifier Number (GLIDE), the Sigma, etc.[62,63], and the Global Earthquake Model Earthquake Consequences Database (GEMECD)[64,65]. Currently, there are many datasets describing landslides caused by individual earthquakes and global inventories of earthquake-induced landslides; however, there are few datasets that comprehensively describe the number of fatalities caused by earthquake-induced landslides, especially for earthquakes in China. The statistics of casualties in historical earthquakes may include only total casualties, but the different causes and numbers of casualties have not been divided in detail. This also makes it difficult for different models to obtain specific analysis results of the relationship between landslides and deaths; at the same time, it is difficult to ensure high accuracy for the evaluation results.

Therefore, this article, which is based on data from the Mainland China Composite Earthquake Causing Casualties Database (MCCEC-DAT)[66,67], collected mortality data for different intensities of 61 historical earthquakes since 1966 and analyzed the relationship between the number of earthquake secondary landslides and the mortality rate, as shown in Table 1. The historical earthquake data with more than 4 different intensity mortality rates, a total of 13 historical earthquake data points, were combined with secondary landslide data (such as landslide density) at each intensity.

Method

Calculation of lethality level

The number of deaths caused by earthquakes is actually a function of earthquake intensity and mortality rate. After an earthquake, different intensity areas will have different mortality rates due to the combined effects of building damage and secondary disasters, and relevant models and methods are based on the proportion of building damage and the mortality rates of different intensities; however, for different intensity areas, the mortality rate caused by different lethal factors is also different, and finding the difference between the mortality rates of various factors is also key.

After an earthquake occurs, damage to buildings, secondary geological disasters, and untimely road congestion may directly or indirectly cause casualties. Based on the actual earthquake situation, the casualties caused by the earthquake are the result of the combined action of various factors in the disaster area after the earthquake, and there is a certain correlation between the comprehensive characteristics of the area reflected

No.	Location	Time	Magnitude (Mw)	Death toll (person)	Mortality rate of each intensity					
					VI	VII	VIII	IX	X	XI
1	Yunnan, Dongchuan	19,660,205	6.5	305			0.00191682	0.00832774		
2	Yunnan, Tonghai	19,700,105	7.8	15,621	0.000119	0.001687	0.015838	0.039332	0.155483	
3	Yunnan, Daguan	19,740,511	7.1	1308	0.000236	0.000608	0.004897	0.03454		
4	Hebei, Tangshan	19,760,728	7.8	262,000			0.0444615	0.09417	0.153	0.22
5	Yunnan, Mohei	19,790,315	6.8	12	0.000039	0.00014	0.00052	0.000742		
6	Yunnan, Lancang-Gengma	19,881,106	7.6	748	0.000014	0.0001	0.001253	0.009378		
7	Sichuan, Batang	19,890,416	6.7	8	0.00005945	0.00055659	0.0029			
8	Sichuan, Shimian	19,890,609	5.2	1		0.0005				
9	Sichuan, Xiaojin	19,890,922	6.6	1		0.00052632				
10	Chongqing, Jiangbei	19,891,120	5.2	3		0.00042644				
11	Jiangsu, Changshu	19,900,210	5.1	2	0.00017513					
12	Qinghai, Gonghe	19,900,426	7	119	0.00041532	0.00258065	0.0035	0.01725		
13	Gansu, Tianzhu	19,901,020	6.2	2			0.0006949			
14	Shanxi, Datong	19,910,326	5.8	1		0.00108696				
15	Hebei, Tangshan	19,910,530	5.1	2		0.00012492				
16	Yunnan, Yongsheng	19,921,218	5.4	1	0.00020747					
17	Xinjiang, Hejing	19,930,203	5.4	4	0.00021505					
18	Xizang, Lazi	19,930,320	6.6	2			0.0025974			
19	Yunnan, Xhongdian	19,930,717	5.6	1	0.00053763					
20	Xinjiang, Kashi	19,931,201	6	2		0.00019646				
21	Xinjiang, Wusu	19,950,502	5.8	2	0.00021482					
22	Gansu, Yongdeng	19,950,722	5.8	10	0.00000278	0.00002762	0.00096502			
23	Yunnan, Wuding	19,951,024	6.5	50	0.00000559	0.00003211	0.00016165	0.00111111		
24	Yunnan, Lijiang	19,960,203	7	309	0.00004609	0.00026963	0.00078037	0.00257959		
25	Sichuan, Yibin	19,960,228	5.4	1		0.0002584				
26	Xinjiang, Jiashi	19,960,319	6.4	24			0.00017225			
27	Yunnan, Lijiang	19,960,702	5.2	2	0.0000186					
28	Yunnan, Lijiang	19,960,925	5.7	1		0.00012484				
29	Sichuan, Baiyu	19,961,225	5.5	2		0.00016978				
30	Xinjiang, Jiashi	19,970,121	6.4	12		0	0.00059084			
31	Xinjiang, Jiashi	19,970,301	6	1		0.0001199				
32	Xinjiang, Jiashi	19,970,406	6.3	8		0	0.00018579			
33	Hebei, Zhangbei	19,980,110	6.2	49		0.00002597	0.00303			
34	Yunnan, Ninglang,	19,981,119	6.2	5	0.00001245	0.00004933	0.00108992			
35	Gansu, Wendeng	19,990,415	4.7	1		0.00344828				
36	Sichuan, Mianzhu	19,991,130	5	1	0.00007622					
37	Henan, Neixiang	20,000,429	4.7	1	0.00001171					
38	Yunnan, Wuding	20,000,821	5.1	2	0.00003165					
39	Sichuan, Yajiang	20,010,223	6	3		0.00004419	0.00050125			
40	Yunnan, Shidian	20,010,410	5.9	3	0.00000251	0.00000835	0.00007391			
41	Sichuan, Yanyuan	20,010,524	5.8	1		0.00010256				
42	Yunnan, Shidian	20,010,608	5.3	1	0.00001255					
43	Yunnan, Yongsheng	20,011,027	6	1		0.00005274				
44	Xinjiang, Kashi	20,030,224	6.8	268	0.0000195	0.000087	0.000389	0.00174		
45	Yunnan, Dayao	20,030,721	6.2	16		0	0.000125984			
46	Neimenggu, Balinzuoqi	20,030,816	5.9	4		0	0.00023613			
47	Xizang, Linzhi	20,030,818	5.7	2		0.0007874				
48	Yunnan, Dayao	20,031,016	6.1	3		0	0.00042553			
49	Gansu, Minle	20,031,025	6.1	10		0	0.000787			
50	Yunnan, Ludian	20,031,115	5.1	4		0.00011608				
51	Xinjiang, Kashi	20,031,201	6.1	10	0.00020521					
52	Neimenggu, Dongwuzhumuqinqi	20,040,324	5.9	1		0.00033445				
53	Sichuan, Yibin	20,040,617	4.7	1	0.00002129					
54	Yunnan, Ludian	20,040,810	5.6	4	0.00000255	0.0053				

Continued

No.	Location	Time	Magnitude (Mw)	Death toll (person)	Mortality rate of each intensity					
					VI	VII	VIII	IX	X	XI
55	Sichuan, Wenchuan	20,080,512	8	69,227	0.00000781	0.00006902	0.00056894	0.00757822	0.07731237	0.24416366
56	Sichuan, Wenchuan(gansu)	20,080,512	8	375	0.000005	0.000107	0.000363	0.001031		
57	Yunnan, Yiliang	20,120,907	5.7	81	0.000005	0.000078	0.0353			
58	Sichuan, Lushan	20,130,420	7	196	0.00000489	0.00003286	0.00029	0.0017055		
59	Gansu, Minxian	20,130,722	6.6	95	0.00000162	0.0002344	0.000625			
60	Yunnan, Ludian	20,140,803	6.5	617	0.00001693	0.00017945	0.00184314	0.015504141		
61	Sichuan, Jiuzhaigou	20,170,808	7.0	29+	0.000002	0.000005	0.006	0.0047		

Table 1. Mortality rate by intensity of 61 historical earthquakes.

Lethality Level			Mortality rate by intensity					
Grade		Interval range	VI	VII	VIII	IX	X	XI
A	0%	0–5%	0.0000001	0.000002	0.00006	0.0004	0.0039	0.07
B	10%	5–15%	0.0000002	0.000004	0.00009	0.0006	0.0063	0.1
C	20%	15–25%	0.0000004	0.000009	0.00013	0.001	0.01	0.14
D	30%	25–35%	0.0000006	0.000013	0.00019	0.0017	0.017	0.15
E	40%	35–45%	0.0000008	0.000016	0.00028	0.0028	0.028	0.18
F	50%	45–55%	0.0000012	0.00002	0.0004	0.0046	0.046	0.21
G	60%	55–65%	0.000006	0.00004	0.0006	0.0076	0.077	0.24
H	70%	65–75%	0.000008	0.00009	0.0008	0.0099	0.099	0.26
I	80%	75–85%	0.000009	0.00013	0.0012	0.0129	0.13	0.27
J	90%	85–95%	0.000012	0.00017	0.0018	0.017	0.17	0.29
K	100%	95–100%	0.000016	0.00024	0.0026	0.022	0.22	0.31

Table 2. The basic lethality matrix applicable nationwide based on the history data.

by these various factors and the possible casualties in the area, based on the previous research results of the author, we carried out a fitting analysis of the mortality rate of each intensity based on the historical earthquake data in Chinese Mainland, on the basis of the proportion of building damage, combined with the factors such as the indoor rate and the lethality level of area, and obtained the fitting relationship between each factor and the mortality rate. The main consideration is that during the investigation of actual earthquakes, it was found that there is a large relationship between the indoor rate and population density and the casualties. At the same time, there is no positive correlation between the proportion of building damage and the casuality, and under the influence of different building types, under the same damage state, there are large differences in the probability of death caused by different types of buildings. Therefore, if the fitting is only based on the proportion of building damage, it will inevitably cause large errors, to reduce errors, we used the lethality level as a coefficient for fitting. The indoor rate and building damage ratio data are mainly determined based on historical earthquake data, and the relevant detailed introduction has been explained in the author's previous research results[68–72]. To obtain the lethality level of each historical earthquake area, this paper selects various influencing factors, such as the indoor rate, population density, earthquake occurrence time and lethality level, to adjust and improve the fitting model, as shown in Eq. 1:

$$\log \mathrm{RD} = 12.479 \times (\mathrm{P_t} \times \rho \times \mathrm{RA} \times \alpha)^{0.1} - 13.3 \quad (1)$$

Where RD is the mortality rate (the ratio of the number of deaths to the total population), RA is the collapse and damage rate of buildings in the disaster area, α is the overall lethality level in the earthquake area, ρ is the population density in the earthquake area, and Pt is the coefficient of the average indoor rate (that is, the average proportion of people inside the building during the earthquake occurrence period).

On this basis, the lethality level of the area can be calculated. We divided the country into 11 levels from 0–100%[68,69,71,72]. Based on the grading of the 11 levels, a lethality matrix was constructed through a comprehensive analysis of the mortality rate at each intensity, as shown in Table 2. In fact, this article mainly conducted further research based on previous studies. In the process of constructing the lethality matrix, the author of this article provided a detailed description and construction process. We conducted analysis based on historical earthquake data, as shown in Table 1. In historical earthquakes, not all intensities have mortality data. However, through the collection and fitting analysis of mortality rates for different intensities of historical earthquakes in different regions, magnitudes, and times, it was found that the distribution intervals of mortality rates for different intensities are relatively fixed, and the differences in mortality rates between adjacent intensities also have characteristics, with differences ranging from 3 to 16 times. At the same time, through the fitting analysis of the mortality rates of each historical earthquake with different intensities, it was found that the fitting

results showed obvious characteristics, the fitting results of the mortality rates of earthquakes located in different regions and with different magnitudes showed similar trends, based on the analysis of all historical earthquakes, the fitting results showed grouping characteristics, to achieve quantitative calculation, linear fitting was carried out, and historical earthquakes were grouped based on the fitting results, on the basis of grouping, calculations were carried out using the multiple relationship between adjacent intensities to obtain the calculation results of the mortality rates of each intensity, in this way, the calculation of lethality levels can be achieved. When determining the overall lethality level of an area, it is possible to determine the mortality rate under different intensities in the area. This grading and mortality rate of each intensity represent the comprehensive level of the region; in fact, it also covers the mortality rate caused by secondary geological disasters in different regions under the same lethality level. Although the overall mortality rate of different intensity levels may be the same, there may be large differences in the causes. Death may be caused by building damage, secondary geological disasters, or both, but regardless of the reason, the mortality rate caused by the destruction of buildings and secondary landslide are all included in this overall mortality rate.

Calculation of the seismic landslide probability level

After an earthquake occurs, for different causes of death, if the calculation is directly based on the mortality rate in the matrix, it may cause errors. In fact, the physical geomorphological environment of an area, such as elevation, relative relief, slope, aspect, land use, lithology, engineering rock group (ERG), distance to river (DTR), normalized difference water index (NDWI), normalized difference vegetation index (NDVI) and annual cumulative rainfall (ACR), can also reflect the overall characteristic level of an area. For different areas, this level can actually correspond to the mortality rate of a group of each intensity; if this level is related to the probability of a secondary landslide, it is possible to rapidly calculate secondary landslide casualties. The probability of the occurrence of coseismic landslides in a region (P_{cols}) can be defined as the total area of coseismic landslides in the region (A_{cols}) divided by the total area of the region (A_{all}).

$$P_{cols} = A_{cols}/A_{all} * 100\% \tag{2}$$

where A_{cols} is the total area of all coseismic landslides and A_{all} is the area of the entire study area (effects of sampling intensity and nonslide/slide sample ratio on the occurrence probability of coseismic landslides).

This paper considers statistics and fitting analysis to obtain the basic distribution characteristics of the mortality rate at different intensities, and on this basis, a correlation analysis of the mortality rate at different intensities and the probability of secondary earthquake landslides was carried out. The quantitative results of the probability of secondary landslides affecting the change in mortality at different intensities were obtained, which laid the foundation for the construction of a lethality matrix considering the effects of secondary earthquake landslides.

Results

In fact, after the earthquake, the actual situation of deaths caused by various factors in the disaster area was comprehensively reflected in the mortality rate, and earthquakes of different regions and magnitudes are affected by population size, population density, etc., resulting in large differences in mortality rate. Therefore, this article first conducts a statistical analysis of the mortality rate in different intensities of 61 historical earthquakes. The results show that the multiple in mortality rate of adjacent intensity is generally between 3 and 16, and the average value is approximately 10[70]. As shown in Fig. 1, although there is a large difference in multiples of each adjacent intensity, the mortality rate of the low-intensity area is large, and the high-intensity is small, but overall, the difference multiple of each adjacent intensity is still within a relatively concentrated range.

As shown in Fig. 2, through the exponential fitting analysis of the mortality rate of more than 3 intensities in historical earthquakes, it is found that even for earthquakes of different regions with different magnitudes, the distribution of the mortality rate by intensity still has obvious characteristics, increasing with increasing intensity. Taking intensity VIII as a separation interval, in the area below intensity VIII, the distribution of the fitted curve is stable, but in the area above intensity VIII, the mortality rate changes with intensity are particularly obvious, the curve changes rapidly, and the mortality rate of the intensity above VIII is significantly greater than the intensity below VIII. This mortality rate includes not only the cause of building damage but also other factors, such as secondary landslides caused by earthquakes. If the assessment of casualties is based solely on factors such as the building damage ratio, it may cause larger errors.

As shown in Fig. 3, through the fitting analysis of 13 historical earthquake data for more than 4 intensities, it is found that the fitting results of earthquakes with different magnitudes in different regions show similar change characteristics, the mortality rate shows a clear increasing trend with increasing intensity, and the fitting curve results show obvious grouping. The fitting curves of different earthquakes in the same group show the same change trends, such as the Tonghai earthquake in 1970 and the Ludian earthquake in 2014, but the proportion of building damage and the actual number of deaths in the area above intensity VIII of the two earthquakes are quite different. That is, for different earthquake regions, the geological and geomorphic environment, population, population density, and building damage ratio may be completely different; correspondingly, there will be a large difference in the mortality rate by intensity. Generally, secondary geological disasters such as landslides and mudslides are more likely to occur in the area above intensity VIII, which may be one of the reasons for the large difference in mortality rate. Through the statistical analysis of the mortality rate with different intensities in historical earthquakes, it is found that the difference in the mortality rate in the areas above and below intensity VIII is relatively obvious; in the area below intensity VIII, the secondary geological disasters are relatively less common, the fitting curve of the mortality rate is relatively stable, and there will not be a large difference in the

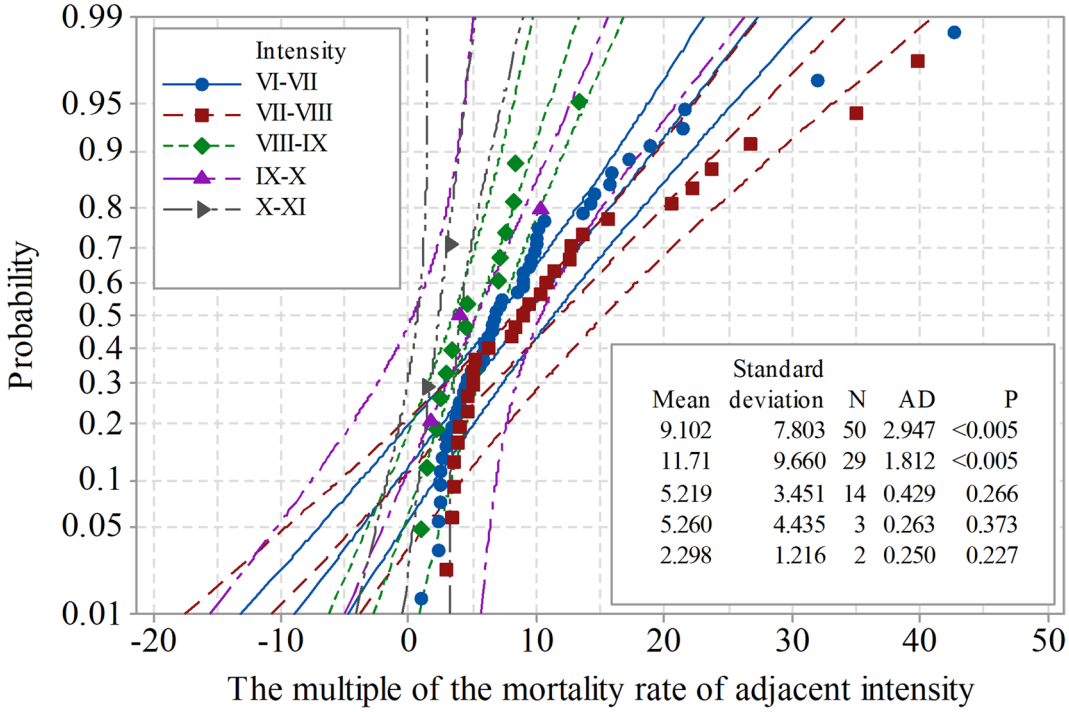

Fig. 1. The distribution characteristics of the multiple relationship of the mortality rate of the adjacent intensity. (Among them, AD is a normality test, which checks whether the data conforms to a normal distribution; by analyzing the normal distribution of multiples of adjacent intensities, the distribution probability of multiples was obtained. The different symbols in the figure represent the multiples of mortality rates of adjacent intensities, and the curve represents the 95% confidence interval.).

mortality rate between adjacent intensities. In the area above intensity VIII, the difference is relatively obvious, and the slope of the fitting curve changes obviously.

As shown in Fig. 4, there is an obvious sudden change in the fitting results of the two ranges above and below intensity VIII. In fact, the slope of the fitting curve below intensity VIII of each earthquake is small, and the distribution is stable. Although different earthquakes have great differences in magnitude, building damage ratios, population density, etc., the difference between the fitting results for the range below intensity VIII is not large; in contrast, the fitting results for the range above intensity VIII show obvious differences, and the fitting results of earthquakes in different regions and different magnitudes are obviously different. Moreover, this difference is not completely positively correlated with magnitude; in other words, the change characteristics are not only affected by earthquake factors such as magnitude but also related to other influencing factors such as geography, landform conditions, secondary geological disasters, population density, etc.

As shown in Table 3, for earthquakes in different regions and with different magnitudes, there is still a clear difference between the slopes of the fitting curves for intensities VI-VII and VIII. Generally, for intensities VI-VII, the slopes of the fitted curves are less than 0.00001, and for those above intensity VIII, the slopes of the fitted curves are generally between 0.001 and 0.008. The distribution ranges of the slopes of the fitting curves of different magnitudes are different, but there is a relatively concentrated range, although the distributions of the slopes of the fitting curves in the two intervals have their own concentrated distribution intervals.

As shown in Fig. 5, there is a significant difference in the multiple relationships of the slope of the fitted curve. The fitting result R^2 value is 0.6781, which is good; generally, as the magnitude increases, the multiple of the difference also shows an increasing trend. For earthquakes below magnitude 7.0, the difference in multiples is less than 100, while for earthquakes above magnitude 7.0, the difference in multiples is relatively obvious, between 400 and 1500; however, this situation is not absolute. There are also cases where the magnitude is large but the multiple is small; for example, for the magnitude 7.1 earthquake in Daguan, Yunnan, the multiple is 42, which is smaller than the magnitude 7.0 earthquake in Lijiang, Yunnan (the multiple is 79), and it is also smaller than the magnitude 6.5 earthquake in Ludian, Yunnan (the multiple is 66); therefore, it is not possible to rely only on the magnitude of the earthquake to realize the distribution characteristics analysis of the mortality rate by intensity. In fact, the reasons for such differences are very complicated, and the main reason may be secondary landslides.

However, earthquake causality data are available only in aggregated form. Based on the current statistical data, it is not possible to obtain the number of deaths caused by secondary landslides of each intensity, and it is difficult to carry out quantitative analysis of the mortality rate based on secondary landslides. Therefore, based on the fitting results of intensity VI-VII, we can obtain the mortality rate results of each intensity (VI-XI) through calculation. Because this result is based on the calculation results of intensity VI-VII, which can theoretically

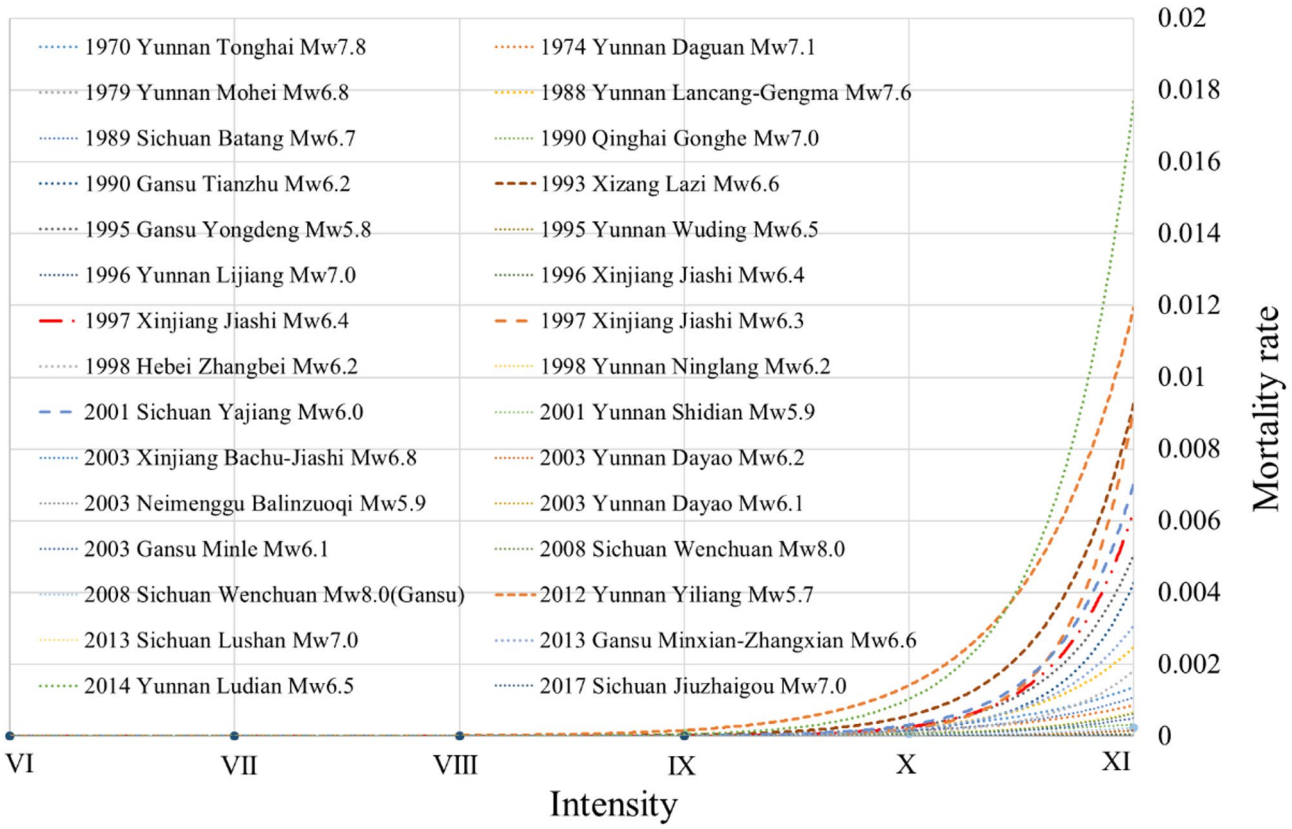

Fig. 2. Exponential fitting results of the mortality rate of more than 3 sub-intensities.

be considered the mortality rate based only on building damage; in this way, the mortality rate data with each intensity level corresponding to building damage in historical earthquakes are obtained, and based on the overall mortality data for each intensity, combining the multiple results of the areas above and below intensity VIII, the mortality rate in the area above intensity VIII is obtained. This mortality rate represents the result of death caused by nonbuilding damage, that is, the mortality rate caused by factors such as secondary geological disasters. The specific calculation method is mainly based on the comprehensive lethality matrix constructed in the early stage. Based on the mortality rate of different intensity corresponding to each lethality level, this article compares and analyzes the mortality rates above and below intensity VIII, and find the corresponding relationship between them. On the basis of fitting the multiple relationship of the results, the calculation is carried out. Since there is no relationship between the mortality rate below intensity VII in historical earthquake data and secondary landslides (this result is obtained based on the analysis of historical earthquake data), that is to say, the mortality rate below intensity VII represents the mortality rate caused by building damage, as well as the comprehensive mortality rate corresponding to the intensity. According to the linear fitting analysis results, there should be a linear relationship between the mortality rate of areas above intensity VIII and areas below intensity VII. However, the actual results have a certain multiplier relationship with each other, which has an amplification effect. Therefore, based on the results of intensity VI-VII, using the multiplier relationship and combining with the previously determined lethality matrix, the results of the range above intensity VIII degrees are obtained through calculation. In the calculation process, the mortality rates of different intensity corresponding to each earthquake are calculated separately according to the lethality level. Therefore, based on the difference between the slopes of the fitting curves in each historical earthquake case, combined with the density of secondary landslides within the corresponding intensity range, we carried out quantitative calculations on the expanding effect of secondary landslides on the mortality rate. The results show that the distribution of the fitting results between the density of secondary landslides and the mortality rate of each intensity shows a certain correlation, and the results are shown in Table 4.

As shown in Fig. 6, based on the distribution results of landslide density within each intensity, it can also be found that the intensity of the earthquake has a positive correlation with the density of secondary landslides; the greater the intensity is, the greater the density. However, the impacts of secondary landslides on the mortality rate with different intensities are different, the number and density of landslides are relatively small in areas below intensity VIII. In the area above intensity VIII, the number of landslides shows an obvious increasing trend, and the density is relatively high since the number of earthquakes with an intensity above X is relatively small. Based on the current results, the results in the intensity IX area are relatively representative, and both the number and the density of landslides are much greater than other intensities.

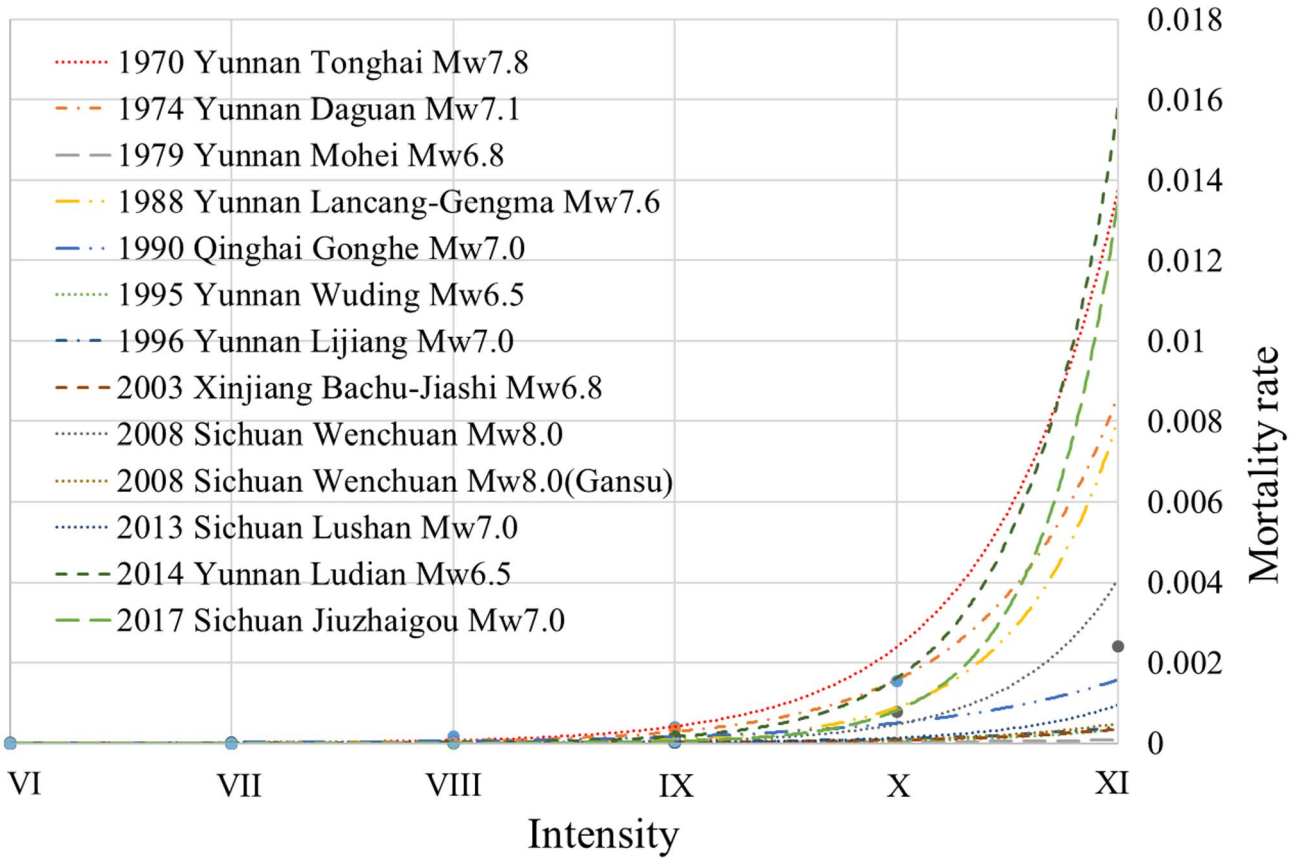

Fig. 3. The exponential fitting results of the mortality rate by intensity of the 13 earthquakes.

Figure 7 shows that, except for the Sichuan Lushan earthquake, the population density decreased with increasing intensity. One of the main reasons for this trend is that the epicenter of the Lushan earthquake was mainly an urban area, and the population density was relatively large. However, at the overall results of individual earthquakes, the population density decreased with increasing intensity, which was also significantly different from that of secondary landslides, while the population density distribution was affected by the size of the regional population. In fact, the population density may also be affected by other factors, such as the location of the earthquake, especially the distribution range of each intensity.

There is a certain correlation between the density of secondary landslides and the population density at each intensity; the greater the density of secondary landslides is, the lower the corresponding population density is, and there is a negative correlation. According to the correlation analysis with the intensity, the landslide density and population density exhibit obvious intensity correlations, as shown in Fig. 8.

As shown in Fig. 9, we selected the number of landslides, landslide density, population density and intensity area to carry out the fitting analysis of the mortality rate of each intensity; for the number of landslides, the greater the number of earthquake landslides is, the greater the possibility of mortality, but not necessarily. Similarly, for the landslide density, this relationship is obvious. The greater the landslide density is, the higher the mortality rate, especially for high-intensity areas. For population density and intensity area, there is a certain negative correlation to the mortality rate, and the area and population of high-intensity areas are relatively small, but the corresponding mortality rate is larger. Similarly, the relationship between the intensity area and the mortality rate is not obvious; the population density and the intensity area have difficulty reflecting the impact of earthquake-induced landslides and other secondary disasters on the mortality rate, and the landslide density can better reflect the relevant characteristics.

On this basis, parameters such as magnitude, intensity, and landslide density were selected for fitting analysis, and a model for the mortality rate with different intensities based on magnitude, intensity and landslide density was obtained. Based on the multiple relationships of the fitting curve of each earthquake obtained in this paper, we calculated and obtained the mortality rate of each intensity corresponding to the corresponding secondary landslide, as shown in Eq. 3.

$$R_i = 0.0024 - 0.0003Mw - 0.0001I + 0.0185LD_i \quad (3)$$

Where R_i is the mortality rate in the range of intensity i, M is the earthquake magnitude, I is the seismic intensity (VIII-XI), and LD_i is the earthquake secondary landslide density in intensity range i.

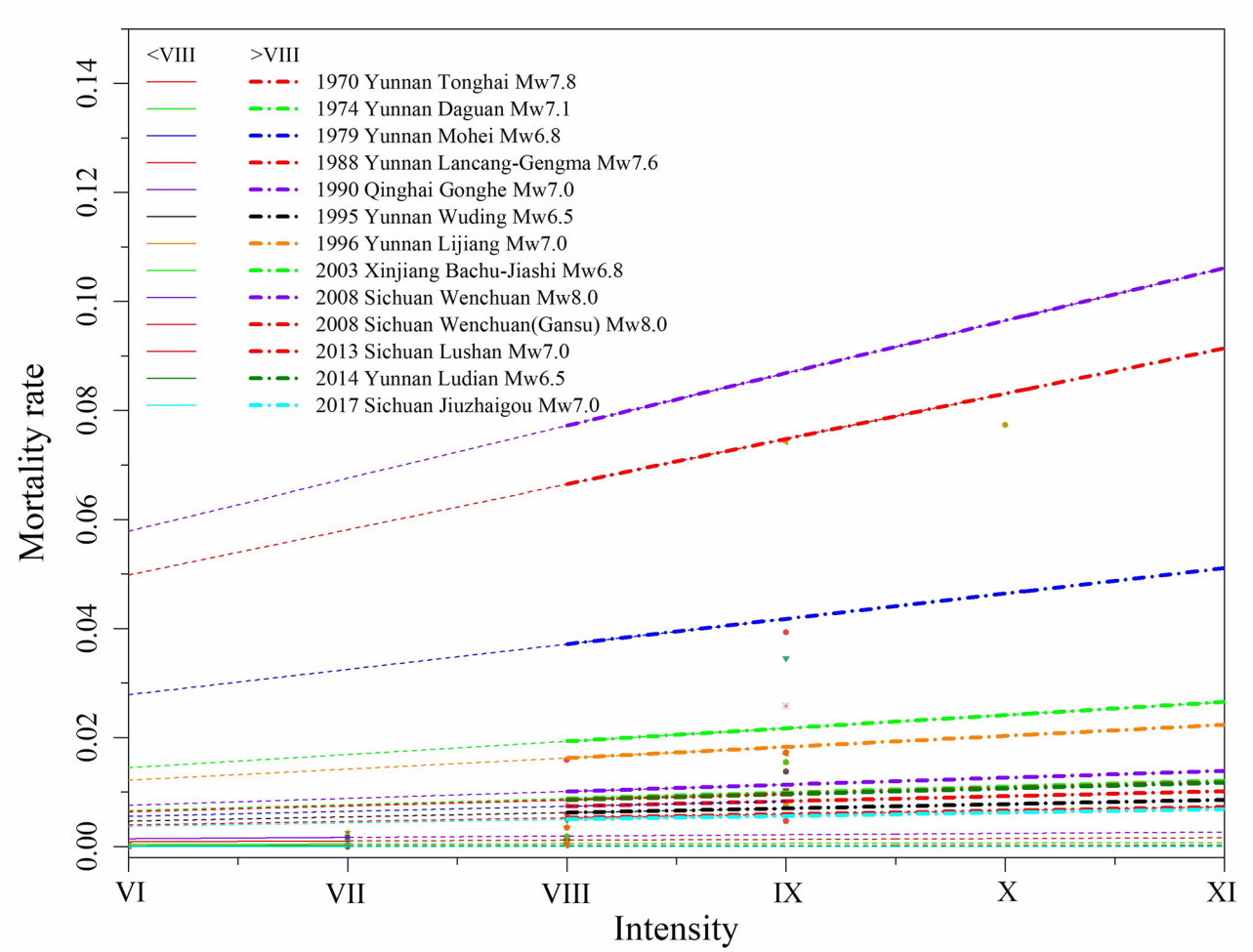

Fig. 4. The segmented linear fitting results of the mortality rate of the 13 earthquakes. (Among them, for comparative analysis, the fitting results below intensity VIII are represented by solid lines, and the fitting results in the area above intensity VIII are represented by dashed lines. Similarly, the fitting results above intensity VIII are also represented in the same way, and the points in the figure are mainly the mortality of intensities.).

The correlation coefficient R of the fitting result is 0.8191, the R^2 is 0.6813, the chi-square coefficient is 0.0016, the F-statistic (F-statistic) is 48.93, the fitting result is relatively good, and it can reflect the relationship between the intensity of the landslide density and the mortality rate.

As shown in Fig. 10, based on the validation results, the model is found to be effective. According to the comparative analysis of the actual mortality rate and the predicted mortality rate, the correlation coefficient R of the fitting results is 0.8423, the R^2 coefficient is 0.7095, the Adj R^2 coefficient is 0.6969, and the standard error of the estimate is 0.0015.

On the premise that the lethality level of each historical earthquake area is determined, we can update and calculate the mortality rate of each intensity corresponding to each area, for example, the lethality level of the Wenchuan earthquake is 60% (group G), that of the Ludian earthquake is 100% (group K), that of the Jiuzhaigou earthquake is 40% (group E), that of the Luding earthquake is 75% (group I), and that of the Jishishan earthquake is 65% (group H). According to the level of these historical earthquakes and the mortality rate of each intensity, based on the multiple relationships of adjacent intensities, the corresponding lethality matrix is constructed, as shown in Table 5. The secondary landslide lethality matrix is still divided into 11 levels from 0 to 100%, the mortality data of each intensity under different levels are obtained, and it mainly refers to the mortality rate of secondary landslides; among them, the mortality rate of each grade VI-VII is basically the same as the comprehensive lethality matrix, and the mortality rate of each intensity above VIII is obtained by calculation. In this way, on the premise of determining the lethality level of a region, the corresponding evaluation calculation can be carried out based on the matrix.

As shown in Table 6, combined with the population numbers of each intensity in historical earthquakes, we verified the accuracy of the matrix. On the premise of determining the lethality level of each earthquake, the error of the calculation results of the overall death data in each earthquake is within ± 50%. In particular, the assessment results of casualties caused by secondary landslides are relatively good, and the general error is within

No.	Earthquake	Magnitude(Mw)	Intensity range	Slope of fitted curve	Multiple
1	Tonghai, Yunnan	7.8	VI-VII	0.0000147330	564.04
			VIII-X	0.0083100000	
2	Daguan, Yunnan	7.1	VI-VII	0.0000567290	42.48
			VIII-IX	0.0024100000	
3	Mohei, Yunnan	6.8	VI-VII	0.0001428200	32.56
			VIII-IX	0.0046500000	
4	Lancang-Gengma, Yunnan	7.6	VI-VII	0.0000022400	412.69
			VIII-IX	0.0009244410	
5	Gonghe, Qinghai	7.0	VI-VII	0.0000241841	52.11
			VIII-IX	0.0012600000	
6	Wuding, Yunnan	6.5	VI-VII	0.0000303890	25.63
			VIII-IX	0.0007788410	
7	Lijiang, Yunnan	7.0	VI-VII	0.0000254582	79.74
			VIII-IX	0.0020300000	
8	Kashi, Xinjiang	6.8	VI-VII	0.0000095412	115.29
			VIII-IX	0.0011000000	
9	Wenchuan, Sichuan	8.0	VI-VII	0.0000062353	1547.64
			VIII-XI	0.0096500000	
10	Wenchuan, Sichuan(Gansu)	8.0	VI-VII	0.0000009165	720.11
			VIII-IX	0.0006599600	
11	Lushan, Sichuan	7.0	VI-VII	0.0000030510	350.71
			VIII-IX	0.0010700000	
12	Ludian, Yunnan	6.5	VI-VII	0.0000159700	66.37
			VIII-IX	0.0010600000	
13	Jiuzhaigou, Sichuan	7.0	VI-VII	0.00000055	1132.29
			VIII-IX	0.00062276	

Table 3. The slope multiplier relationship of the mortality rate fitting curve for different intensities of historical earthquakes.

±30%; that is, the mortality rate with different levels of intensity obtained based on the density of secondary landslides after the earthquake can be more accurate, as shown in Fig. 11.

Discussion

Based on the fitting analysis, the distribution of mortality by intensity has obvious characteristics: the difference in the mortality rate between adjacent intensities is between 3 and 16, and the average is approximately 10. For earthquakes located in different regions and with different magnitudes, the fitted curves show a positive correlation with intensity, which also provides a basis for the assessment of the number of casualties based on the mortality rate by intensity.

The reasons for the rapid changes in the mortality rate at different intensities may include many factors. According to the analysis of historical earthquakes, the number of casualties caused by secondary geological disasters induced by earthquakes is also relatively large, especially in areas above intensity VIII, and the number and density of secondary landslides are much greater than those in areas below intensity VIII.

As shown in Table 7, the deaths caused by historical earthquakes were not only caused by the destruction of buildings, for example, the large-scale landslide induced by the earthquake caused approximately 20,000 deaths and missing persons. In the Yushu earthquake in 2010, the number of deaths caused by secondary geological disasters was also more than 10%. In the Yiliang earthquake in 2012, the total number of deaths were 81, of which 59 were caused by secondary geological disasters, accounting for more than 50% of the deaths. The Ludian earthquake in 2014 caused 617 deaths, and the number of deaths caused by secondary geological disasters was approximately 250, accounting for 40.52%. In the Jiuzhaigou earthquake in 2017 caused 29 deaths, of which only 4 were due to the destruction of buildings, and the remaining 25 were mainly due to the secondary geological disasters caused by the earthquake, accounting for 80%. The proportion of the number of deaths caused by secondary geological disasters is relatively high. In some earthquakes, the number of deaths is far greater than the number of deaths caused by damage to buildings; however, if the calculation of the number of deaths is based only on the proportion of building damage, it will inevitably cause a large error.

However, due to the limitations of historical conditions, the current statistics on earthquake deaths are only comprehensive data within an intensity range, and there are no classification statistics based on the number of deaths caused by building damage or secondary geological disasters. This may also cause large errors due to the lack of consideration of geological hazards. This paper attempts to analyze historical earthquakes comprehensively based on the segmental fitting results of the mortality rate of different intensities and combined with secondary landslide data to construct a casualty assessment method considering secondary disasters.

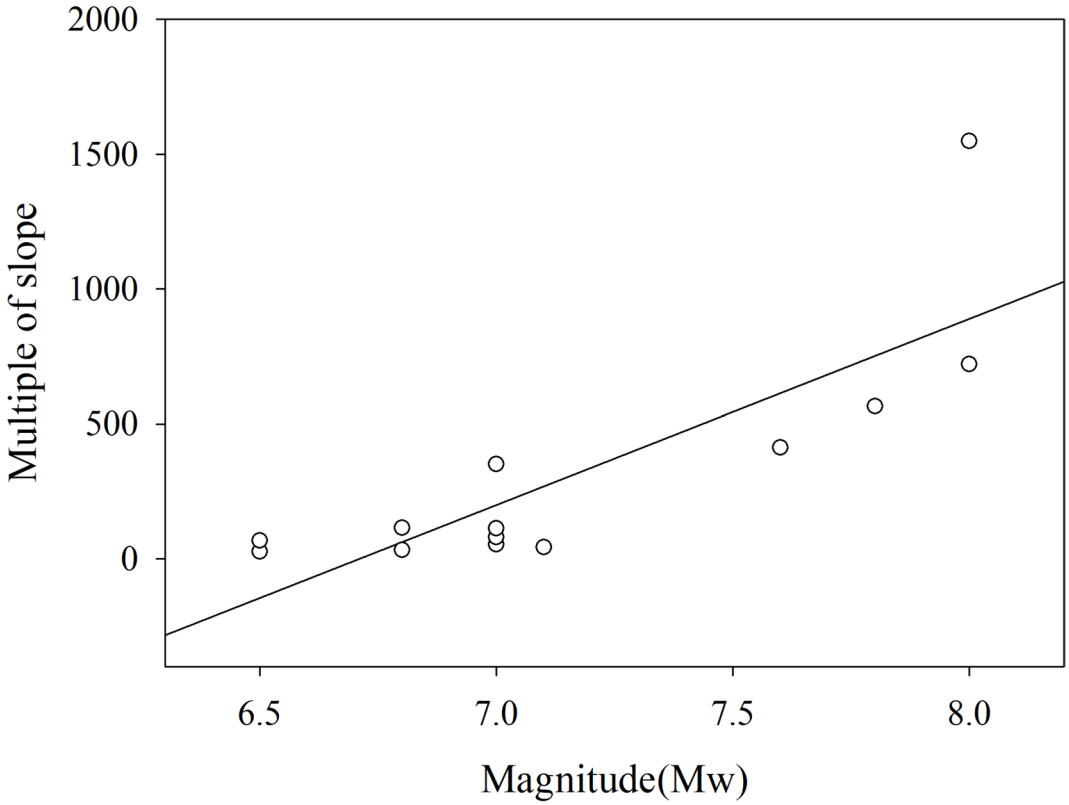

Fig. 5. The distribution of the relationship between the slope multiple of the fitted curve and the magnitude.

In fact, the number or density of secondary landslides with different intensities also has a greater impact on the mortality rate, based on the relevant literature, it is found that the density changes of different earthquake intensities are also quite different, such as the Wenchuan earthquake, due to its large magnitude and wide range of influence, caused a relatively large number of earthquake disasters, and different scholars obtained different results on the number of secondary geological disasters, for example, some scholars have found through remote sensing interpretation of 39 counties (cities) of the Wenchuan earthquake that secondary geological disasters are mainly concentrated in the area above the intensity VIII, that there were 5093 landslides and landslide clusters caused by the earthquake, with a total area approximately 958 km^2, the proportion of secondary landslides in each intensity (VI-XI) is 0.81%, 15.94%, 23.09%, 24.9%, 21.36% and 13.9%, respectively[73–83], the area proportion of the collapse in the VII-XI region are 0.7%, 13.1%, 13%, 30%, and 43.2%, respectively[84], the surface damage rate caused by the high seismic intensity area is much larger than that of the low intensity area[85], and the density of secondary geological hazards decreases as the intensity decreases, the law of its distribution has a good correlation with the seismic intensity level[86].

Although the results of earthquake secondary landslides obtained by different scholars may vary, in general, the secondary landslides in the Wenchuan earthquake-stricken area are mainly distributed in intensity zones VIII-XI, and the landslide density and volumes are basically consistent with the attenuation of seismic intensity. The distribution of large and medium-sized landslides is related to the high-intensity areas in the meloseismic region[87]; therefore, as shown in Table 4, on the basis of related research, this paper combines the results of many researchers to obtain the landslide densities of each intensity (VI-XI) of the Wenchuan earthquake, which are distributed as 0.001 pcs/km^2, 0.007 pcs/km^2, 0.131 pcs/km^2, 0.13 pcs/km^2, 0.3 pcs/km^2, and 0.432 pcs/km^2. The slope of the fitting curve for the mortality rate of the Wenchuan earthquake is 0.0000062353 for intensity VI-VII and 0.00965 for above intensity VIII. The multiples of the slopes of the fitted curves differ by a factor of 1547, which also shows similar variation characteristics to the landslide density.

For the Yushu earthquake, the number of earthquake-induced landslides, collapses, and debris flows were mainly distributed in the intensity areas above VII, and the number of geological disasters increased sharply near the high-intensity areas. Among them, there were 161 areas with intensity IX, accounting for 47%, and there were 76 and 58 geological disasters in regions VII and VIII, accounting for 22% and 17%, respectively, and the degree of landslide and collapse damage was not as obvious as that in high-intensity areas[88–92]; therefore, as shown in Table 4, based on the results of many researchers, the degree of landslide density of each intensity (VI-IX) of the Yushu earthquake was 0.05 pcs/km^2, 0.1 pcs/km^2, 0.68 pcs/km^2, 1.23 pcs/km^2. An overall feature of the Yushu earthquake landslide distribution is that it is relatively concentrated in the IX intensity, which is much greater than other intensity areas, and the average landslide density in the area above the intensity VIII is also larger than that in the area below the intensity VIII.

Earthquake	Attributes	Intensity					
		VI	VII	VIII	IX	X	XI
Wenchuan, Sichuan	Number of landslides (pieces)	29	571	827	892	765	498
	Landslide density (pieces/km^2)	0.001	0.007	0.131	0.13	0.3	0.432
	Population (person)	76,688,578	26,888,769	4,227,933	1,118,141	139,371	167,259
	Intensity area (km^2)	314,906	84,449	27,786	7738	3144	2419
	Population density (person/km^2)	243.5285	318.4025	152.1605	144.5	44.3292	69.14386
Yushu, Qinghai	Number of landslides (pieces)	48	76	58	161		
	Landslide density (pieces/km^2)	0.05	0.1	0.68	1.23		
	Population (person)	78,504	34,150	27,575	11,143		
	Intensity area (km^2)	22,423		7030	992		
	Population density (person/km^2)	5.024038		3.922475	11.23286		
Yiliang, Yunnan	Number of landslides (pieces)	33	63	57			
	Landslide density (pieces/km^2)	0.02	0.09	0.22			
	Population (person)	948,797	197,557	32,919			
	Intensity area (km^2)	2642	792	263			
	Population density (person/km^2)	359.1207	249.4407	125.1673			
Lushan, Sichuan	Number of landslides (pieces)	273	365	384	151		
	Landslide density (pieces/km^2)	0.021	0.091	0.271	0.726		
	Population (person)	1,711,672	596,746	383,779	53,196		
	Intensity area (km^2)	13,059	4078	1424	211		
	Population density (person/km^2)	131.0722	146.333	269.5077	252.1137		
Minxian-Zhangxian, Gansu	Number of landslides (pieces)	60	90	154			
	Landslide density (pieces/km^2)	0.004964	0.024725	0.21813			
	Population (person)	1,112,831	414,151	66,422			
	Intensity area (km^2)	12,086	3640	706			
	Population density (person/km^2)	92.07604	113.7777	94.08215			
Ludian, Yunnan	Number of landslides (pieces)	235	197	192	99		
	Landslide density (pieces km^2)	0.04	0.12	0.66	1.1		
	Population (person)	1,407,063	234,576	27,872	7737		
	Intensity area (km^2)	8390	1580	290	90		
	Population density (person/km^2)	167.7072	148.4658	96.11034	85.96667		
Jiuzhaigou, Sichuan	Number of landslides (pieces)	20	69	138	45		
	Landslide density (pieces/km^2)	0.011	0.027	0.18	0.306		
	Population (person)	1,513,854	142,169	23,362	4006		
	Intensity area (km^2)	14,006	3372	778	139		
	Population density (person/km^2)	108.0861	42.16163	30.02828	28.82014		

Table 4. The number and density of secondary landslides associated with historical earthquakes.

The magnitudes of the 5.7 and 5.6 earthquakes in Yiliang, Yunnan were relatively small; however, due to the influence of geological and geomorphological conditions, secondary landslides are relatively common. Among these events, the number of secondary landslides caused by earthquakes is 15,357 in the area of intensity VIII, accounting for 37.3%, 63 in the area of intensity VII, accounting for 41.2%, and 33 in the area of intensity VI, accounting for 21.6%. The number of secondary landslides of each intensity is concentrated in the area above intensity VII. Due to the large difference in the area of different intensities, the density of secondary landslides of each intensity is quite different, as shown in Table 4. Among them, the intensity VIII area is 0.22 pcs/km^2, the intensity VII is 0.09 pcs/km^2, the intensity VI is 0.02 pcs/km^2, and the density of secondary landslides above intensity VIII is quite different from that in the area below VIII[93–95]. This finding is consistent with the distribution characteristics of casualties, which are actually concentrated in the area of intensity VIII.

As shown in Table 4, the distribution of this density shows similar characteristics; the greater the intensity is, the greater the density of secondary landslides, and the slope of the fitting curve for the mortality rate of the Lushan earthquake is 0.000003051 for intensity VI-VII, the distribution characteristics of the various intensities of landslides during the 2013 Lushan earthquake were similar to those during the Wenchuan earthquake. Among them, there are 2227 landslides in the area of intensity IX, 4695 in the area of intensity VIII, 6848 in the area of intensity VII, and 1754 in the area of intensity VI; if the statistics are only based on the number, the number of the range below the VIII is greater than the number of the range above, among which the number of new disaster points of IX is 151, the number of VIII is 384, the number of VII is 365, the number of VI is 273, and the number of new disaster sites in the area below the VIII is also greater than that in the area above VIII[96–100]. Regardless of the number of landslides of each intensity or the number of new additions of each intensity, the landslides in the

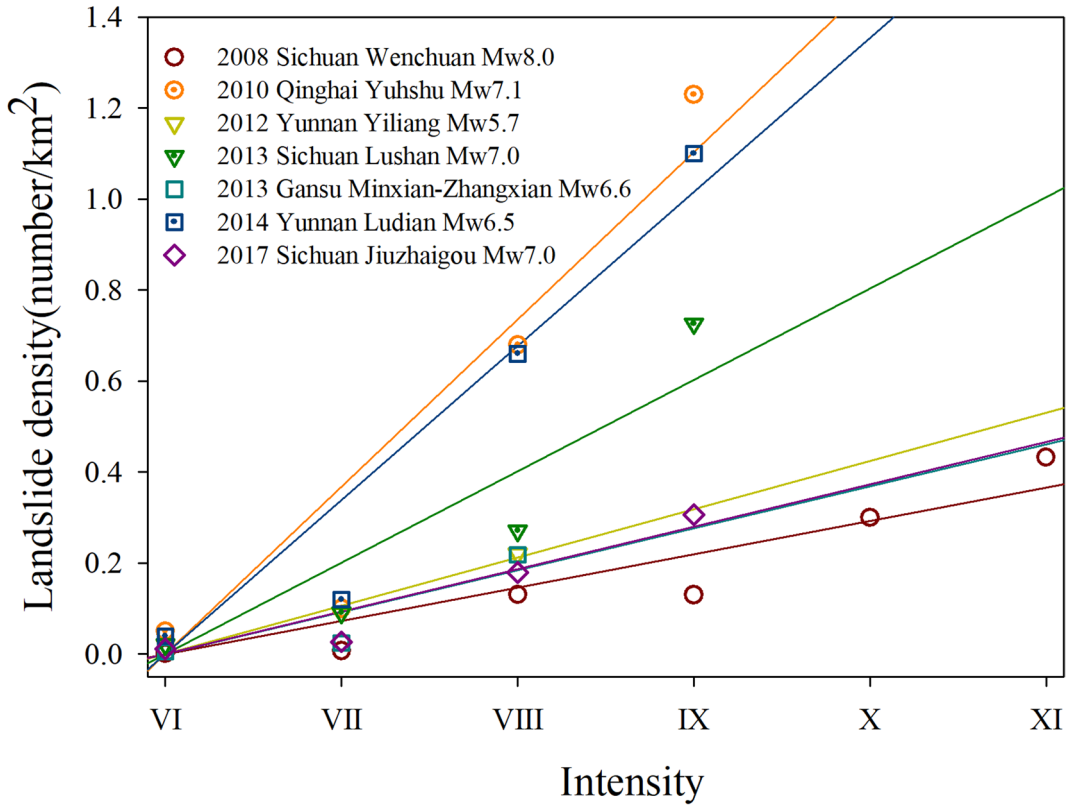

Fig. 6. Distribution relationship of landslide density with different intensities.

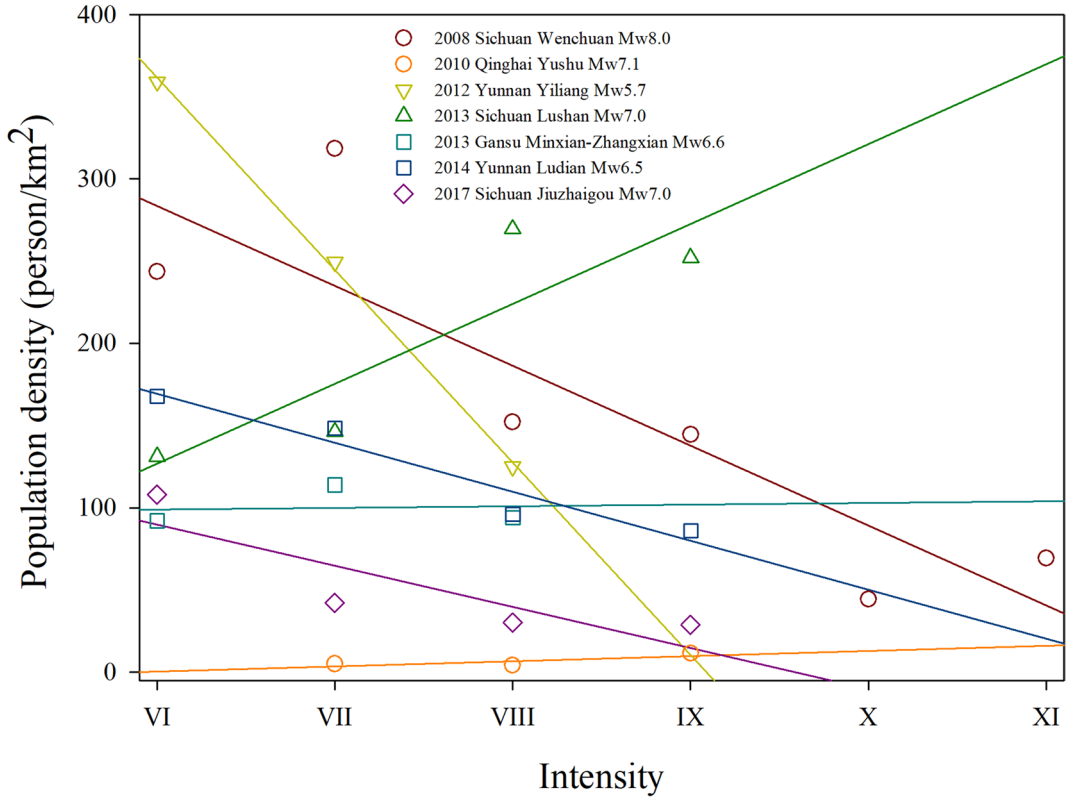

Fig. 7. Distribution relationship of landslide density with different intensities.

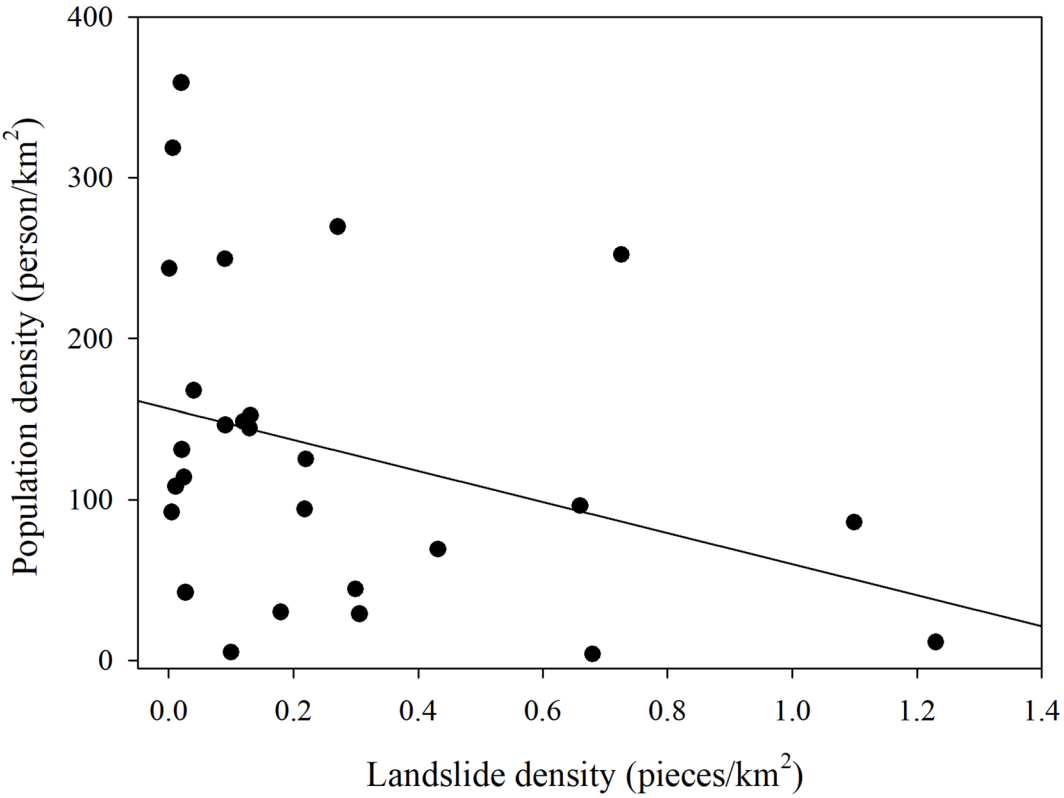

Fig. 8. Correspondence between secondary landslide density and population density.

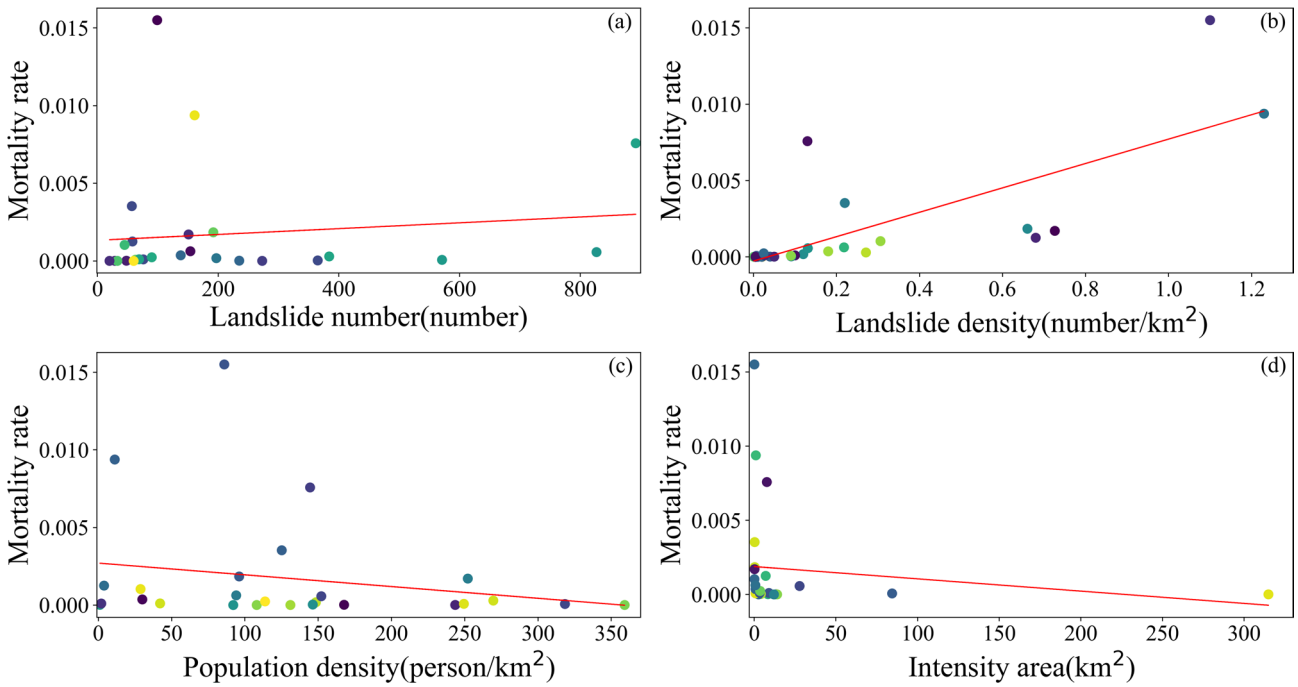

Fig. 9. The distribution relationship between the mortality rate with different intensity and different influencing factors. (The different colors of data points represent different seismic intensity data.).

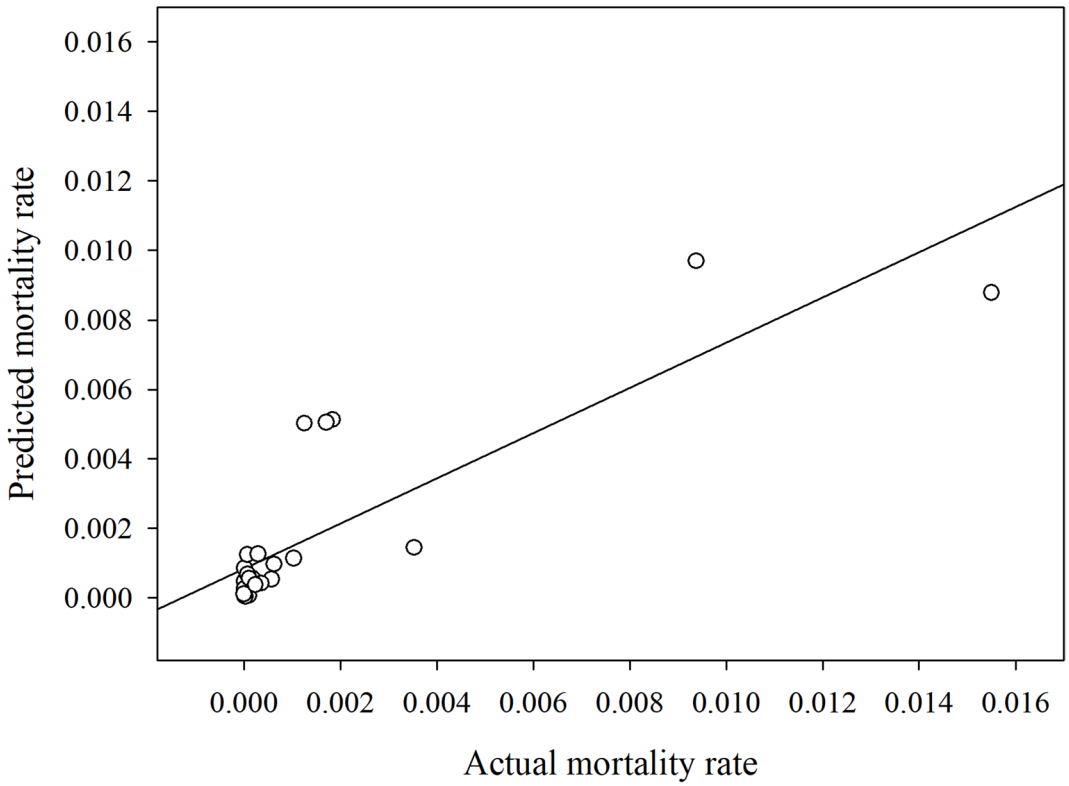

Fig. 10. Comparative analysis of actual mortality rate and predicted mortality rate.

Lethality Level			Mortality rate by intensity					
Grade		Interval range	VI	VII	VIII	IX	X	XI
A	0%	0–5%	0.000000100	0.000002000	0.000053150	0.000013548	0.001433088	0.012932110
B	10%	5–15%	0.000000150	0.000003500	0.000063230	0.000024702	0.003578106	0.017478230
C	20%	15–25%	0.000000250	0.000006000	0.000074512	0.000031106	0.007716837	0.023622463
D	30%	25–35%	0.000000600	0.000009000	0.000091151	0.001194447	0.010300801	0.031926623
E	40%	35–45%	0.000000800	0.000016000	0.000179300	0.001290100	0.013750000	0.043150000
F	50%	45–55%	0.000001200	0.000020000	0.000204598	0.001393413	0.018354155	0.058318805
G	60%	55–65%	0.000006000	0.000040000	0.000313500	0.001505000	0.024500000	0.068820000
H	70%	65–75%	0.000007800	0.000080000	0.000566039	0.001843924	0.029492270	0.078872967
I	80%	75–85%	0.000010000	0.000150000	0.000892798	0.003953407	0.049855040	0.091002081
J	90%	85–95%	0.000012000	0.000170000	0.001029890	0.006407506	0.071118168	0.099129890
K	100%	95–100%	0.000014950	0.000220000	0.001310000	0.009000000	0.095014500	0.117400000

Table 5. Lethality matrix considering the secondary landslides resulting from earthquakes.

		Actual number of deaths			Secondary landslide deaths		
Earthquake	Lethality Level(%)	Actual death (person)	Calculation result (person)	Error (%)	Actual death (person)	Calculation result (person)	Error (%)
Sichuan, wenchuan	60	69,227	63444.04	8.35	20,000	21141.9	−5.71
Qinghai, yushu	70	2698	1405.81	47.89	270	234.28	13.23
Yunnan, yiliang	80	81	73.72	8.98	60	57.03	4.95
Gansu, minxian	10	95	99.31	−4.54	15	12.49	16.77
Yunnan, ludian	100	617	321.49	47.89	250	201.83	19.27
Sichuan, jiuzhaigou	40	29	26.84	7.43	20	15.74	21.29
Sichuan, luding	75	93	68.758	−26.07	51	35.94	−29.53
Gansu, jishishan	65	151	112.56	−25.46	35	25.52	−27.09

Table 6. The results of the number and density of secondary landslides in historical earthquakes.

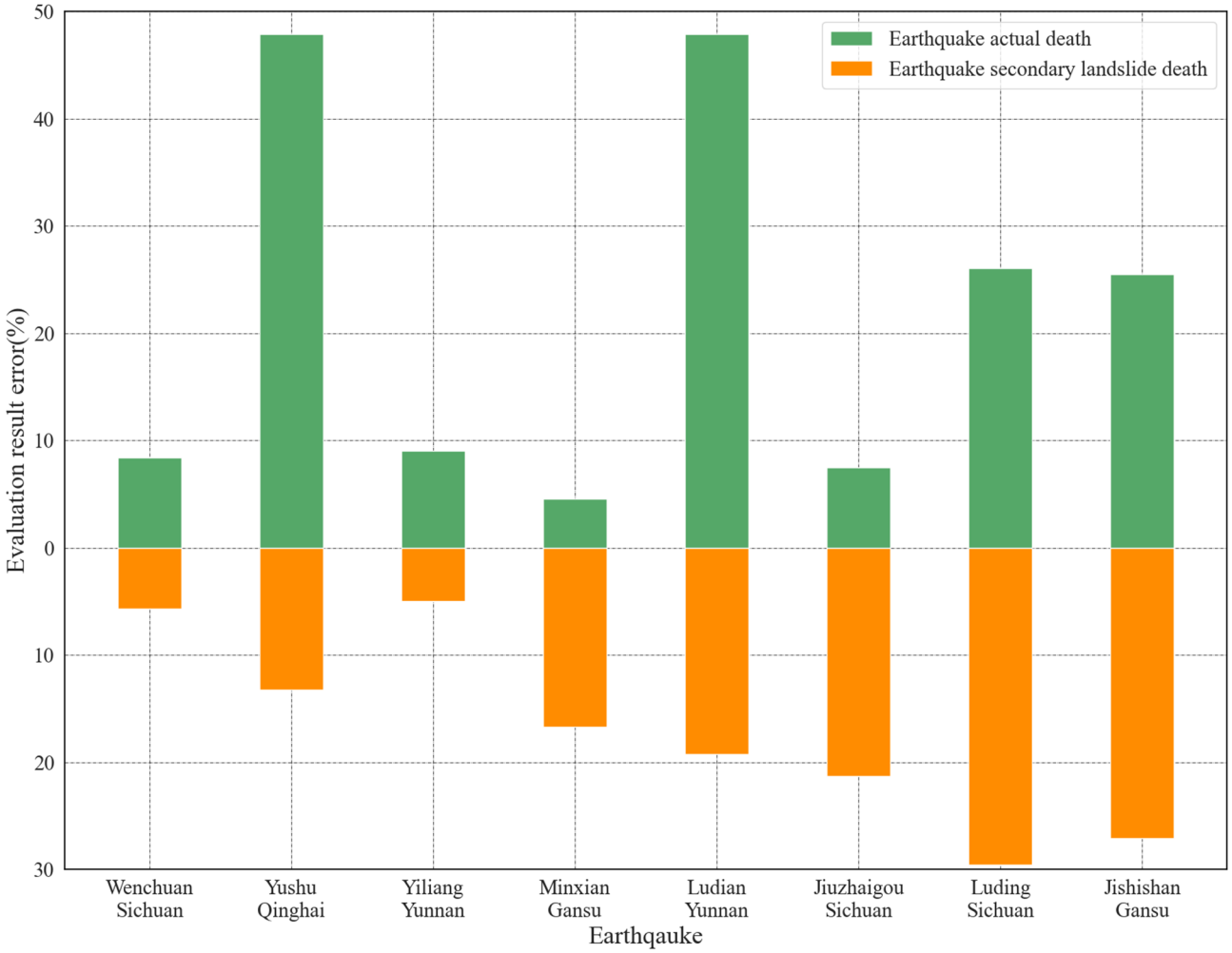

Fig. 11. Error analysis of actual death and assessment results.

areas below the VIII may be more serious than those in the above areas. However, through comparative analysis, it is found that the intensities of IX-VI are quite different; the intensities of IX-VI are 208, 1418, 6848, and 13,027, respectively; the disaster point densities of IX-VI are 10.7 pcs/km^2, 3.31 pcs/km^2, 1.7 pcs/km^2, and 0.135 pcs/km^2, respectively; and the densities of the newly added disaster points of each intensity (IX-VI) are 0.726 pcs/km^2, 0.271 pcs/km^2, 0.091 pcs/km^2, and 0.021 pcs/km^2[101–107].

Overall, the Minxian-Zhangxian earthquake in 2013 triggered at least 2330 landslides, with an overall landslide density of 7.06 km^2[108–110]. Overall, the landslides were mainly concentrated in area VIII; therefore, as shown in Table 4, through statistical analysis, the landslide densities of each intensity (VI-VIII) were 0.004964 pcs/km^2, 0.024725 pcs/km^2, and 0.21813 pcs/km^2, respectively. Additionally, the density difference of different intensities was greater, the average landslide density in the area above intensity VIII was 0.0148 pcs/km^2, that below intensity VIII was 0.218 pcs/km^2, the multiple differences were approximately 15, and the landslide density and mortality rate showed relatively obvious correlations.

For example, for the magnitude 6.5 earthquake in Ludian, Yunnan on August 3, 2014, the highest intensity is IX, and landslides occur at each intensity. The distribution characteristics are very obvious. The density of secondary landslides is positively correlated with the seismic intensity[111–115]. The intensity increases, the density increases. The area of intensity IX is 90 km^2, and the number of geological disaster points is 99, including 3 superlarge and 6 large-scale disaster points, such as the Hongshiyan dammed lake, Ganjiazhai landslide, and Wangjiapo landslide. The area of intensity VIII is 290 km^2, and the number of geological disaster points is 192, including 6 large-scale disaster points. The area of intensity VII is 1580 km^2, and the number of geological disaster points is 197, including 1 large disaster point. The area of intensity VI is 6548 km^2, and the number of geological disaster points is 235. The density of geological disasters of each intensity of VI-IX is 0.04 pcs/km^2, 0.12 pcs/km^2, 0.66 pcs/km^2, and 1.1 pcs/km^2, as shown in Table 4.

The highest intensity of the Jiuzhaigou earthquake is IX. Based on the comparison of remote sensing images before and after the 1883 landslides were visually interpreted, the interpretation results showed that the types of earthquake disasters were mainly small and medium-sized shallow landslides and collapses[116]. Among them, the number of newly added disaster points with an intensity of VI is 20, the intensity of VII is 69, the intensity

No.	Location	Magnitude (Mw)	Time	Number of deaths (person)	Deaths caused by landslides (person)	Proportion (%)	Description
1	Yunnan, Tonghai	7.8	19,700,115	15,621			More than 30 landslides occurred in the extreme earthquake area, most of which were located in the north of the Qujiang River (Accurate and detailed data are not given yet)
2	Yunnan, Daguan	7.1	19,740,511	1423	73(part)	5.13	Earthquake-induced landslides and other disasters caused the whole village to be buried in Shoupayan Village, and none of the residents were spared
3	Yunann, Mohei	6.8	19,790,315	11	2	18.18	The phenomenon of landslides is sporadically distributed, mainly with intensity VIII-IX, such as the landslide near Menjing, etc.
4	Yunan, Lancang-Gengma	7.6	19,881,106	748			In areas with intensity above VIII, secondary disasters such as landslides are more common, and they are mostly distributed in bands (Accurate and detailed data are not given yet)
5	Qinghai, Gonghe	7	19,900,426	119			Landslides occur around Longyangxia Reservoir (Accurate and detailed data are not given yet) (Liu et al., 1990)
6	Yunnan, Wuding	6.5	19,951,024	52			52 dead, 808 seriously injured, 13,007 slightly injured in earthquake (Accurate and detailed data are not given yet)
7	Yunnan, Lijiang	7	19,960,203	309			Disasters such as landslides are mainly concentrated in the yulong snow mountain and its eastern slope. The landslides buried some roads and caused traffic interruptions, etc. (Accurate and detailed data are not given yet)
8	Yunnan, Yanjin	5.1	20,060,722	22	20	90.91	From Jili to Dousha in Daguan County, rolling stones, collapses and landslides are common, 20 killed by rolling stones or collapse
9			20,060,825				
10	Sichuan, Wenchuan	8	20,080,512	69,227	Approximately 20,000	28.89	Approximately 20,000 people dead and missing in earthquake-induced massive landslide
11	Qinghai, Yushu	7.1	20,100,414	2698	270	10.01	The total death toll exceeded 3000, of which many landslides occurred after the earthquake, which directly impacted residential areas
12	Yunnan, Yiliang	5.7	20,120,907	81	59	72.84	The total death toll was 81, mostly from rolling stones and landslides
13	Sichuan, Lushan	7	20,130,420	196	24	12.24	After the earthquake, some landslides occurred in the mountains, hitting the villages
14	Gansu, Minxian-Zhangxian	6.6	20,130,722	95	15	15.79	Secondary disasters such as landslides occurred in Yongguang Village
15	Yunnan, Ludian	6.5	20,140,803	617	250	40.52	Many landslides occurred, and some villages built on the hillside fell with the landslide, resulting in many casualties
16	Sichuan, Jiuzhaigou	7	20,170,808	25	Approximately 20	80	There are few deaths due to building damage, most of them are due to secondary geological disasters

Table 7. Statistics of deaths caused by secondary landslides in historical earthquakes.

of VIII is 138, the intensity of IX is 45, and the newly added geological disaster points are mainly concentrated in the area above intensity VIII, with a total of 183 points, accounting for 67.28% of all earthquake areas. With increasing earthquake intensity, the density of newly added disaster points also gradually increases, especially in the areas above and below intensity VIII. The density of newly added disaster points is obviously different, and there is an order of magnitude difference[117]. As shown in Table 4, based on the results of many researchers, the secondary landslide density of each intensity (VI-IX) is 0.011 pcs/km^2, 0.027 pcs/km^2, 0.18 pcs/km^2, 0.306 pcs/km^2, through the analysis of historical earthquakes, it is found that for earthquakes of different magnitudes in different regions, the distribution characteristics of secondary landslides are relatively obvious; for areas with intensities of VI-VII, the landslide density is relatively small; for areas with intensities above VIII, the density of secondary landslides significantly increases, and the difference between the multiples of the average density in the two regions is generally greater than 10. This characteristic of change is highly consistent with the increase in the mortality rate.

Through the analysis of the secondary landslide data of historical earthquakes, it is found that the number of earthquakes in different regions and of different magnitudes exhibit similar trends. As the intensity increases, the number of secondary landslides does not necessarily increase, but rather the density increases. According to the comparative analysis of the mortality rate with different intensities, the two areas above and below intensity VIII exhibit multiple obvious relationships, and this change is closely related to the density of secondary landslides. Secondary landslides exhibit a very obvious increase in the mortality rate. Based on the fitting results of VI-VII, the mortality rate with different intensities above VIII is obtained. Combined with the difference between this mortality rate and the comprehensive mortality rate, the secondary landslides mortality rate of each intensity level is obtained, and based on these results, it is possible to carry out a fitting analysis and obtain mortality data with different intensities based on landslide densities.

On the basis of the mortality data of different intensities combined with the lethality levels of historical earthquake regions, we constructed a lethality matrix of secondary landslides, with which each lethality level corresponds to the mortality data of a group of intensities. This mortality rate represents the probability of death caused by secondary landslides and can also achieve rapid assessment of casualties from secondary disasters. Based on the verification of historical seismic data, the error of the evaluation results can generally be guaranteed

to be within ± 50%. Among them, the Wenchuan earthquake, the Ludian earthquake and the Jiuzhaigou earthquake are the basic data for constructing the matrix, and the verification results based on the 3 earthquakes are not representative; however, according to the calculation results of the Yushu earthquake, Yiliang earthquake and Minxian earthquake, the error is still very small, within ± 30%, which can further verify the validity of the matrix. At the same time, in order to further verify the effectiveness of the secondary landslide lethality matrix, we also selected the Luding earthquake in 2022 and the Jishishan earthquake in 2023 for verification, and the error between the calculated results and the actual results was within ± 30%.

This mortality rate is significantly different from the overall mortality rate of the region, and the mortality rate caused by building damage can provide a feasible idea for carrying out casualty assessment of secondary landslides. The lethality matrix of landslides constructed based on this can better reflect the mortality rate of different levels in different regions. Based on historical seismic data, we verified the matrix. On the premise of determining the lethality level of each historical earthquake area, the error between the calculated result and the actual number of deaths can be guaranteed to be within ± 50%, which also provides a more feasible idea for the rapid assessment of casualties of earthquake secondary landslides. Although the calculation results of each earthquake are basically smaller than the actual number of deaths, one of the main reasons is that the mortality rate of each lethality level in the matrix is a calculation result, and there may still be a difference in the actual mortality rate; therefore, the mortality data in the matrix also need to be adjusted and updated based on new data and methods in future work.

In fact, this landslide density is a probability of earthquake-induced secondary landslides; to a certain extent, the matrix effectively links the occurrence probability of landslides with the earthquake intensity and mortality rate. Thus, in follow-up research, how to establish the relationship between this probability and the lethality level is the main direction and focus of the research. Therefore, we imagine whether it is possible to determine the mortality rate of different causes of death by intensity, and construct a single-factor lethality matrix based on building damage and secondary landslides, etc., or based on this comprehensive matrix, find the change law of secondary landslide mortality relative to comprehensive mortality. This pattern points to changes in the level of regional lethality levels; that is, if an area is at a certain lethality level, then its mortality rate of each intensity is determined. If there is the possibility of secondary geological disasters in this area, it will increase the mortality rate of different intensities in this area, and the increased mortality actually corresponds to other lethality levels. This will also cause a change in the lethality level of area, and since the current matrix describes overall mortality, therefore, how to analyze the mortality rate caused by secondary landslides, the effect of secondary landslides on the mortality rate is the key to constructing a single-factor lethality matrix, which is also the key to rapid assessment of casualties caused by secondary landslides.

Conclusion

The statistics and fitting analysis of the mortality rate in historical earthquakes revealed that with increasing intensity, the mortality rate showed an increasing trend, and the fitting curve of the mortality rate by intensity showed similar variation characteristics. With increasing intensity, the mortality rate rapidly increased, especially in the range above intensity VIII. The change characteristics were obvious. Through the linear fitting of the mortality rate with adjacent intensity, it was found that the distribution characteristics were also obvious in the area above intensity VIII. The slope of the fitting curve could be used for the analysis of the distribution characteristics of the mortality rate.

Based on this, we carried out a group fitting analysis of the historical earthquake mortality data and performed linear fitting on the mortality below and above intensity VIII. The results showed different intensities for different areas and different magnitudes. The fitting curves of different groups showed similar distribution characteristics, and the slopes above intensity VIII were much greater than those below intensity VIII; that is, secondary landslides had a very obvious expansion effect on the mortality rate.

According to the relevant statistics of historical earthquake data collected in this paper, secondary landslides are one of the main reasons for the large difference in mortality. The number of deaths caused by secondary landslides during earthquakes was large, secondary landslides were also concentrated mainly in the range above intensity VIII, the density and intensity showed a positive correlation, and with increasing intensity, the density showed an obvious increasing trend.

Through the quantitative calculation of the mortality rate with different intensities, multiple quantification results of the slope of the fitting curve were obtained, which also provides a basis for the assessment method considering secondary landslides, combined with the landslide density, magnitude, and intensity. The model was constructed, the model fitting result was relatively good, the R^2 coefficient was 0.6813, the deviation between the predicted value and the actual number of deaths was small, and the R^2 coefficient of the fitting result was 0.7095, which further verifies the validity of the model and provides a scientific basis for the casualty assessment method that considers secondary landslides.

Based on the lethality level of each historical earthquake area, we constructed a matrix for secondary landslides and obtained the mortality rate of each intensity corresponding to different lethality levels. Through the verification of historical earthquakes, it was found that the error between the assessment results of death caused by secondary landslides and the actual death can be guaranteed to be within ± 50%. This mortality rate is actually directly related to the probability of earthquake-induced secondary landslides; therefore, to obtain more accurate evaluation results, how to obtain the relationship model between the probability of secondary landslides and the lethality level of an area is important. Therefore, in future work, we will select nine influencing factors for landslides (land use, aspect, engineering rock group (ERG), slope, distance to river (DTR), relative relief, normalized difference water index (NDWI), normalized difference vegetation index (NDVI) and annual cumulative rainfall (ACR)) and, based on the Newmark model, construct a fitting model between the probability

of landslide occurrence and mortality rate (or lethality level) to improve the accuracy of earthquake secondary landslide hazard assessment results.

Data availability

Data is provided within the manuscript.The data that support the findings of this study are available from the corresponding author upon reasonable request.the corresponding author: xiachaoxu@ies.ac.cn.

Received: 21 December 2024; Accepted: 19 June 2025
Published online: 01 July 2025

References

1. Miles, S. & Keefer, B. (ed K, D.) Toward a comprehensive areal model of Earthquake-Induced landslides. *Nat. Hazards Rev.* **10** 1 19–28 https://doi.org/10.1061/(asce)1527-6988(2009)10:1(19) (2009).
2. Keefer, D. K. Landslides caused by earthquakes. *Geol. Soc. Am. Bull.* **95**, 406–421 (1984).
3. Liu, F., Zhang, L., Liu, H., & Zhang, Y. Danger assessment of earthquake induced geological disaster in China. *J. Geomech.* (02),127–131. (2006).
4. Zhang, L., Zhang, Y. & Liu, X. Study on distribution of earthquake secondary geological hazards in China and on their regionalization at city-Level. *J. Disaster Prev. Mitigation Eng.* **29** (03), 356–360 (2009).
5. Kirschbaum, D., Adler, R., Hong, Y., Hill, S. & Lerner-Lam, A. A global landslide catalog for hazard applications: method, results, and limitations. *Nat. Hazards*. **52**, 561–575. https://doi.org/10.1007/s11069-009-9401-4 (2009).
6. Daniell, J. E., Schaefer, A. M. & Wenzel, F. Losses associated with secondary effects in earthquakes. *Front. Built Environ.* **3**, 30. https://doi.org/10.3389/fbuil.2017.00030 (2017).
7. Marano, K. D., Wald, D. J. & Allen, T. I. Global earthquake casualties due to secondary effects: a quantitative analysis for improving rapid loss analyses. *Nat. Hazards*. **52** (2), 319–328. https://doi.org/10.1007/s11069-009-9372-5 (2009).
8. Capolongo, D., Refice, A. & Mankelow, J. Evaluating earthquake-triggered landslide hazard at the 519 basin scale through Gis in the upper Sele river Valley. *Surv. Geophys.* **23**, 595–625. https://doi.org/10.1023/A:1021235029496521 (2002).
9. Del Gaudio, V. & Wasowski, J. Time probabilistic evaluation of seismically induced landslide hazard in Irpinia (Southern Italy). *Soil Dyn. Earthq. Eng.* **24**, 915–928. https://doi.org/10.1016/j.soildyn.2004.06.019 (2004).
10. Del, Gaudio, V., Pierri, P. & Calcagnile, G. Analysis of seismic hazard in landslide-prone regions: criteria and example for an area of Daunia (southern Italy). *Nat. Hazards*. **61**, 203–215. https://doi.org/10.1007/s11069-011-9886-5 (2012).
11. Havenith, H-B., Strom, A., Caceres, F. & Pirard, E. Analysis of landslide susceptibility in the Suusamyr region, Tien shan: statistical and geotechnical approach. *Landslides* **3**, 39–50. https://doi.org/10.1007/s10346-005-0005-0 (2006).
12. Chousianitis, K., Del, Gaudio, V., Kalogeras, I. & Ganas, A. Predictive model of Arias intensity and newmark displacement for regional scale evaluation of earthquake-induced landslide hazard in Greece. *Soil Dyn. Earthq. Eng.* **65**, 11–29. https://doi.org/10.1016/j.soildyn.2014.05.009528 (2014).
13. James, N. & Sitharam, T. G. Assessment of seismically induced landslide hazard for the state of Karnataka using GIS technique. *J. Indian Soc. Remote Sens.* **42**, 73–89. https://doi.org/10.1007/s12524-013-0306-z563 (2014).
14. Kahal, A., Abdelrahman, Alfaifi, H. & Yahya, M. Landslide hazard assessment of the Neom promising city, Northwestern Saudi arabia: an integrated approach. *J. King Saud Univ. - Sci.* **33**, 101279. https://doi.org/10.1016/j.jksus.2020.101279 (2020).
15. Kamp, U., Growley, B. J., Khattak, G. A. & Owen, L. A. GIS-based landslide susceptibility mapping for the 2005 Kashmir earthquake region. *Geomorphology* **101**, 631–642. https://doi.org/10.1016/j.geomorph.2008.03.003 (2008).
16. Kamp, U., Owen, L., Growley, B. & Khattak, G. Back analysis of landslide susceptibility zonation mapping for the 2005 Kashmir earthquake: an assessment of the reliability of susceptibility zoning maps. *Nat. Hazards*. **54**, 1–25. https://doi.org/10.1007/s11069-009-9451-7 (2010).
17. Xu, C. & Xu, X. Xiwei. GIS and ANN model for earthquake triggered landslides susceptibility zonation. *Geol. Sci. Technol. Inform.* **31**(3), 116–121 (2012).
18. Xu, C., Dai, F., Xu, X. & Lee, Y. H. GIS-based support vector machine modeling of earthquake-triggered landslide susceptibility in the Jianjiang river watershed, China. *Geomorphology* 145–146. https://doi.org/10.1016/j.geomorph.2011.12.040 (2012).
19. Xu, C., Xu, X., Yao, X. & Dai, F. Three (nearly) complete inventories of landslides triggered by the May 12, 2008 Wenchuan Mw 7.9 earthquake of China and their Spatial distribution statistical analysis. *Landslides* **11**, 441–461. https://doi.org/10.1007/s10346-013-0404-6 (2013a).
20. Xu, C. et al. Application of an incomplete landslide inventory, logistic regression model and its validation for landslide susceptibility mapping related to the May 12, 2008 Wenchuan earthquake of China. *Nat. Hazards* **68**, 883–900. https://doi.org/10.1007/s11069-013-0661-7 (2013b).
21. Jibson, R. W. Regression models for estimating coseismic landslide displacement. *Eng. Geol.* **91**, 209–218. https://doi.org/10.1016/j.enggeo.2007.01.013 (2007).
22. Li, Z. et al. Quantitative vulnerability Estimation for scenario-based landslide hazards. *Landslides* **7** (2), 125–134. https://doi.org/10.1007/s10346-009-0190-3 (2010).
23. Kirschbaum, D. B. et al. A global landslide catalog for hazard applications: method, results, and limitations. *Nat. Hazards*. **52**, 561–575. https://doi.org/10.1007/s11069-009-9401-4 (2010).
24. Liu, J., Gao, M. & Wu, S. Probabilistic seismic landslide hazard zonation method and its application. *Chin. J. Rock Mechan. Eng.* (35), 3101–3109. (2016).
25. Sangeeta, & Maheswari, B. K. Earthquake Induced Landslide Hazard Assessment of Chamoli District, Uttarakhand, India Using Weighted Overlay Method, India, in *16th European Conference on Earthquake Engineering (16ECEE)* (2018).
26. Meena, S., Ghorbanzadeh, O. & Blaschke, T. A. Comparative study of statistics-based landslide susceptibility models: a case study of the region affected by the Gorkha Earthquake in Nepal. *Int. J. Geo-Information* **8**, 24. https://doi.org/10.3390/ijgi8020094 (2019).
27. Nguyen, B. Q. V. & Kim, Y. T. Regional-scale landslide risk assessment on mt. Umyeon using risk index Estimation. *Landslides* **18** (7), 2547–2564. https://doi.org/10.1007/s10346-021-01622-8 (2021).
28. Hua, Y., Wang, X., Li, Y., Xu, P. & Xia, W. Dynamic development of landslide susceptibility based on slope unit and deep neural networks. *Landslides* **18**(1), 281–302. https://doi.org/10.1007/s10346-020-01444-0 (2021).
29. Kahal, A. Y., Abdelrahman, K., Alfaifi, H. J. & Yahya, M. M. A. Landslide hazard assessment of the Neom promising city, Northwestern Saudi arabia: an integrated approach. *J. King Saud Univ. Sci.* **33** (2), 101279. https://doi.org/10.1016/j.jksus.2020.101279 (2021).
30. Zhuang, J. Q. et al. Risk assessment of collapses and landslides caused by 512 Wenchuan earthquake-a case study of Dujiangyan-Wenchuan highway. *Chin. J. Rock Mechan. Eng.* **29**(S2), 3735–3742 (2010).
31. Tao, S., Deyong, H., Zhao, W. & Wang, F. Y. Susceptibility assessment of secondary landslides triggered by earthquakes: a case study of Northern Wenchuan. *Geographical Res.* **29** (9), 1594–1605 (2010).

32. Bai, X., Dai, Y., Yu, Q. & Shao, W. Risk assessment modeling of earthquake-induced landslides and its preliminary application. *J. Seismol. Res.* **38**(2), 301–312 (2015).
33. Xu, C. et al. GIS-based landslide susceptibility assessment using analytical hierarchy process in Wenchuan earthquake region. *Chin. J. Rock Mechan. Eng.* **28**(s2), 3978–3985 (2009).
34. Wang, X., Nie, G. & Ma, M. Application of multiple ground motion factors in earthquake-induced landslide hazard evaluation. *Acta Seismol. Sin.* **34**(1), 76–84 (2012).
35. Wang, X., Nie, G. & Wang, S. Evaluation criteria of landslide hazards induced by Wenchuan earthquake using fuzzy mathematical method. *Rock. Soil. Mech.* **32** (2), 403–410 (2011).
36. Xu, C. et al. Landslide hazard mapping using GIS and weight of evidence model in Qingshui river watershed of 2008 Wenchuan earthquake struck region. *J. Earth Sci.* **23**, 97–120. https://doi.org/10.1007/s12583-012-0236-7 (2012).
37. Xu, C., Xu, X., Bengang, Z. & Shen, L. Probability of coseismic landslides: a new generation of earthquake triggered landslide hazard model. *J. Eng. Geol.* **27** (5), 1122–1130 (2019).
38. Budimir, M. E. A., Atkinson, P. M. & Lewis, H. G. Earthquake and landslide events are associated with more fatalities than earthquakes alone. *Nat. Hazards.* **72** (2), 895–914. https://doi.org/10.1007/s11069-014-1044-4 (2014).
39. Nadim, F., Kjekstad, O., Peduzzi, P., Herold, C. & Jaedicke, C. Global landslide and avalanche hotspots. *Landslides* **3** (2), 159–173. https://doi.org/10.1007/s10346-006-0036-1 (2006).
40. Godt, J. et al. Rapid assessment of earthquake-induced landsliding, in *Proceedings of the First World Landslide Forum* (United Nations University, Tokyo, Japan, 2008).
41. Nowicki, M. A., Wald, D. J., Hamburger, M. W., Hearne, M. & Thompson, E. M. Development of a globally applicable model for near real-time prediction of seismically induced landslides. *Eng. Geol.* **173**, 54–65. https://doi.org/10.1016/j.enggeo.2014.02.002 (2014).
42. Kritikos, T., Robinson, T. R. & Davies, T. R. H. Regional coseismic landslide hazard assessment without historical landslide inventories: a new approach: coseismic landslide hazard assessment. *J. Geophys. Res. Earth Surf.* **120** (4), 711–729. https://doi.org/10.1002/2014JF003224 (2015).
43. Parker, R. N. et al. Spatial distributions of earthquake-induced landslides and hillslope preconditioning in the Northwest South island, new Zealand. *Earth Surf. Dyn.* **3** (4), 501–525. https://doi.org/10.5194/esurf-3-501-2015 (2015).
44. Robinson, T. R. et al. Rapid postearthquake modeling of coseismic landsliding intensity and distribution for emergency response decision support. *Nat. Hazards Earth Syst. Sci.* **17**(9), 1521–1540 (2017).
45. Froude, M. J. & Petley, D. N. Global fatal landslide occurrence from 2004 to 2016. *Nat. Hazards Earth Syst. Sci.* **18**, 2161–2181 (2018).
46. Zhang, S., Li, C., Zhang, L., Peng, M. & Xu, Q. Quantification of human vulnerability to earthquake-induced landslides using bayesian network. *Eng. Geol.* **265**, 105436. https://doi.org/10.1016/j.enggeo.2019.105436 (2019).
47. Zhang, S. et al. Quantification of human vulnerability to earthquake-induced landslides using bayesian network. *Eng. Geol.* **265**, 105436. https://doi.org/10.1016/j.enggeo.2019.105436 (2020).
48. Zhou, Q., Xu, Q., Zeng, P., Zhao, K. & Yuan, S. Scenario-based quantitative human vulnerability assessment of site-specific landslides using a probabilistic model. *Landslides* **19** (4), 993–1008. https://doi.org/10.1007/s10346-021-01827-x (2022).
49. Petley, D. Global patterns of loss of life from landslides. *Geology* **40** (10), 927–930 (2012).
50. Tanyaş, H. et al. Presentation and analysis of a worldwide database of earthquake-induced landslide inventories. *J. Geophys. Research: Earth Surf.* **122**, 1991–2015. https://doi.org/10.1002/2017JF004236 (2017).
51. Tanyaş, H. et al. Rapid prediction of the magnitude scale of landslide events triggered by an earthquake. *Landslides* **16**, 661–676. https://doi.org/10.1007/s10346-019-01136-4 (2019).
52. Lin, Q. & Wang, Y. Spatial and temporal analysis of a fatal landslide inventory in China from 1950 to 2016. *Landslides* **15**(12), 2357–2372. https://doi.org/10.1007/s10346-018-1037-6. (2018).
53. Lin, J. W., Hsieh, M. H. & Li, Y. J. Factor analysis for the statistical modeling of earthquake-induced landslides. *Front. Struct. Civil Engine.* **14** (1), 123–126 (2020).
54. Valagussa, A., Marc, O., Frattini, P. & Crosta, G. B. Seismic and geological controls on earthquake-induced landslide size. *Earth Planet. Sci. Lett.* **506**, 268–281 (2019).
55. Wang, Y., Lin, Q. & Shi, P. Spatial pattern and influencing factors of landslide casualty events. *J. Geog. Sci.* **28** (3), 259–274 (2018).
56. Fan, X. et al. Rapidly evolving controls of landslides after a strong earthquake and implications for hazard assessments. *Geophys. Res. Lett.* **48**, e2020GL090509. https://doi.org/10.1029/2020GL090509 (2021).
57. Chen, X. L., Li, Yang, H. & Zhao, Q. Y. Numerical simulation of earthquake effects on rock slope. *Acta Petrologica Sinica.* **27** (6), 1899–1908 (2011).
58. Nowicki, J. M. A. et al. A global empirical model for near-real-time assessment of seismically induced landslides. *J. Geophys. Res. Earth Surf.* **123**, 1835–1859. https://doi.org/10.1029/2017JF004494 (2018).
59. Nowicki, Jessee, M. A., Hamburger, M. W., Ferrara, M. R., McLean, A. & FitzGerald, C. A global dataset and model of earthquake-induced landslide fatalities. *Landslides* **17** (6), 1363–1376. https://doi.org/10.1007/s10346-020-01356-z (2020).
60. Khalaj, S. et al. A methodology for uncertainty analysis of landslides triggered by an earthquake. *Comput. Geotech.* **117**, 103262. https://doi.org/10.1016/j.compgeo.2019.103262 (2020).
61. Tonje, G. & Henrik, J. Assessment of data availability for the development of landslide fatality curves. *Landslides* **14** (3), 1113–1126. https://doi.org/10.1007/s10346-016-0775-6 (2017).
62. Tschoegl, L., Below, R. & Guha-Sapir, D. Impacts An Analytical Review of Selected Data Sets on Natural Disasters and Centre for Research on the Epidemiology of Disasters, Brussels, Belgium. (2006).
63. Li, S. H., Luo, X. H. & Wu, L. Z. A new method for calculating failure probability of landslide based on ANN and a convex set model. *Landslides* **18** (8), 2855–2867. https://doi.org/10.1007/s10346-021-01652-2 (2021).
64. So, E. Introduction to the GEM Earthquake Consequences Database (GEMECD). GEM Technical Report, -14 V1.0.0, 158 pp. GEM Foundation, Pavia. https://doi.org/10.13117/GEM.VULN-MOD.TR2014.14 (2014).
65. Bocchini, G. M. et al. New Zealand contributions to the global earthquake model's earthquake consequences database (GEMECD). *Bull. New. Z. Soc. Earthq. Eng.* **48** (4), 245–263. https://doi.org/10.5459/bnzsee.48.4.245-263 (2015).
66. Li, Y., Zhang, Z. & Xin, D. A. Composite catalog of damaging earthquakes for Mainland China. *Seismol. Res. Lett.* **92** (6), 3767–3777. https://doi.org/10.1785/0220210090 (2021).
67. Xia, C. et al. A composite database of casualty-inducing earthquakes in Mainland China. *Nat. Hazards.* **116**, 3321–3351. https://doi.org/10.1007/s11069-022-05811-z (2023).
68. Xia, C. et al. Research on the rapid assessment of earthquake casualties based on the anti-lethal levels of buildings. *Geomatics Nat. Hazards Risk* **11**(1), 377–398. https://doi.org/10.1080/19475705.2019.1710581 (2020).
69. Xia, C. et al. A new model for the quantitative assessment of earthquake casualties based on the correction of anti-lethal level. *Nat. Hazards* **110**(2), 1199–1226. https://doi.org/10.1007/s11069-021-04988-z (2022).
70. Xia, C., Nie, G., Li, H., Fan, X. & Zhou, J. Xiwei, zhou, junxue. Research on correlation between earthquake intensity and mortality rate based on historical earthquake data. *Earthq. Res. China* **38**(1), 153–165 (2022).
71. Nie, G., Xia, C. & Fan, X. Grading of anti-lethal level based on historical earthquake mortality data. *Chin. J. Geol.* **55** (4), 1298–1314. https://doi.org/10.12017/dzkx.2020.078 (2020).
72. Nie, G., Xia, Chaoxu, F. & Li, X. Research on the lethal level of buildings based on historical seismic data. *Chin. J. Geol.* **56** (4), 1250–1266. https://doi.org/10.12017/dzkx.2021.068 (2021).

73. Li, X., Kong, J., Cui, Y. & Tian, S. Statistical relations between landslides induced by Wen Chuan earthquake and earthquake parameters, geological as well as Geomorphological factors. *J. Eng. Geol.* **18**(1), 8–14 (2010).
74. Qi, S., Xu, Q., Liu, J., Zhang, B. & Liu, J. Spatial distribution analysis of landslides triggered by 2008.5.12 Wenchuan earthquake, China. *Eng. Geol.* **116**(1), 95–108. https://doi.org/10.1016/j.enggeo.2010.07.011 (2010).
75. Huang, R. & Li, W. Research on development and distribution rules of geohazards induced by Wenchuan earthquake on 12th may, 2008. *Chin. J. Rock Mechan. Eng.* **27** (12), 2585–2592 (2008).
76. Gao, H., Pei, X., Cui, S., Zhu, L. & Liang, Y. Geological Hazards after Earthquake in Wenchuan Earthquake Area: Distribution and Evolution Features. *J. Yangtze River Sci. Res. Inst.* (08), 73–80 (2019).
77. Xu, C., Dai, F. & Yao, X. Incidence number and affected area of Wenchuan Earthquake-induced landslides. *Sci. Technol. Rev.* **27**(11), 79–81 (2009).
78. Xu, C. et al. Identification and analysis of secondary geological hazards triggered by a magnitude 8.0 Wenchuan earthquake. *J. Remote Sens.* **13**(04), 754–762 (2009).
79. Xu, C., Fuchu, F. & Xiao, J. Statistical analysis of characteristic parameters of landslides triggered by May 12,2008 Wenchuan earthquake. *J. Nat. Disasters* **20**(04), 147–153. https://doi.org/10.13577/j.jnd.2011.0424 (2011).
80. Xu, C. et al. Detailed catalog of landslides triggered by the 2008Wenchuan earthquake and statistical analyses of their Spatial distribution. *J. Eng. Geol.* **21**(01), 25–44 (2013).
81. Xu, C., Dai, F., & Xu, X. Wenchuan Earthquake-induced landslides: an overview. *Geol. Rev.* **56**(06), 860–874. (2010).
82. Xu, C. et al. GIS based certainty factor analysis of landslide triggering factors in Wenchuan earthquake. *Chin. J. Rock Mechan. Eng.* **29**(1), 2972–2980 (2010b).
83. Yuan, R. et al. Density distribution of landslides triggered by the 2008 Wenchuan earthquake and their relationships to peak ground acceleration. *Bull. Seismol. Soc. Am.* **103**(4), 2344–2355 (2013).
84. Guo, Z., Zhou, C., Sun, X. & Zhang, J. The distribution of landslide triggered by Wenchuan earthquake and its causative factors. *Earth Sci. Front.* (05), 234–242 (2010).
85. Sun, X. et al. Assessment and analysis of the secondary geological disasters induced by the 5.12 Wenchuan earthquake. *Acta Geol. Sinica* **84**(09), 1283–1291 (2010).
86. Liang, J. et al. Development and distribution rules of geohazards induced by Wenchuan M8.0 earthquake. *J. Catastrophol* **30**(01), 63–68 (2015).
87. Qiao, J. et al. Shi, lili. A study on characteristics of distribution of Earthquake-induced landslides and hazard zoning. *J. Catastrophology* **24**(02), 25–29 (2009).
88. Peng, L. *Yushu 4.14 earthquake secondary geological disasters in the development and distribution characteristics* (China University of Geosciences, Beijing, 2013).
89. Jiang, Y. Study on Yushu Earthquake Landslides of Qinghai Province, China (China University of Geosciences, Beijing, 2014).
90. Wang, J. et al. Development tendency of Geo-hazards induced by the Yushu Ms7.1 earthquake. *J. Catastrophol* **28**(04), 61–66 (2013).
91. Yin, Y. et al. Research on major characteristics of geohazards induced by the Yushu Ms7.1 earthquake. *J. Eng. Geol.* **18**(03), 289–296 (2010).
92. Xu, C., Xu, X. & Yu, G. Study on the characteristics, mechanism, and Spatial distribution of Yushu earthquake triggered landslides. *Seismology Geol.* **34** (01), 47–62 (2012).
93. Zhang, J. et al. Characteristics of sedondary geological hazards induced by Yiliang 9·07 earthquakes in Yunnan Province. *J. Eng. Geol.* **22**(02), 280–291. https://doi.org/10.13544/j.cnki.jeg.2014.02.015 (2014).
94. Feng, X., Li, Z., Li, X. & Wang, M. Characteristics of geological hazards in Yiliang earthquake and statistical analyses of their Spatial distribution. *Seismology Geol.* **37** (02), 555–564 (2015).
95. Zhang, Y., Li, X., Xie, Y., Yu, J. & Chen, K. Analysis on seismotectonic background and earthquake hazard characteristic in zhaotong,yunnan: taking Ludian MS6.5 earthquake and Yiliang MS5.7、5.6 earthquake as examples. *J. Seismol. Res.* **39**(02), 270–278 (2016).
96. Chen, C. & Hu, K. Comparison of distribution of landslides triggered by wenchuan, Lushan and Ludian earthquakes. *J. Eng. Geol.* **25** (03), 806–814. https://doi.org/10.13544/j.cnki.jeg.2017.03.028 (2017).
97. Tian, S., Kong, J., Xiaoyi, F. & Ding, M. Before and after the Lushan earthquake contrast geohazards in earthquake-stricken areas. *Mountain Res.* **32** (01), 111–116. https://doi.org/10.16089/j.cnki.1008-2786.2014.01.014 (2014).
98. Li, W., Huang, R., Xu, Q. & Tang, C. Rapid prediction of coseismic landslides triggered by Lushan earthquake, sichuan, China. *J. Chengdu Univ. Technol. (Science Technol. Edition)* **40**(03), 264–274 (2013).
99. Xu, C. & Xiao, J. Spatial analysis of landslides triggered by the 2013 Ms7.0 Lushan earthquake: a case study of a typical rectangle area in the Nortneast of Taiping town. *Seismology Geol.* **35** (02), 436–451 (2013).
100. Chen, X., Cui, P., You, Y., Yang, Z. & Kong, Y. Secondary mountain disasters induced by the 4·20 Lushan earthquake and disaster mitigation. *Earth Sci. Front.* **20**(03), 29–34 (2013).
101. Miao, C., Ding, M., Wang, J. & Zhou, P. Distribution characteristics and cause of secondary mountain hazards in Lushan earthquake-stricken area. *Resour. Environ. Yangtze Basin* **23**(11), 1572–1579 (2014).
102. Yang, Z. Features of secondary mountain hazards triggered by the 4·20 Lushan earthquake. *J. Sichuan Univ. (Engineering Sci. Edition)*. **45** (04), 76–83. https://doi.org/10.15961/j.jsuese.2013.04.004 (2013).
103. Li, X. et al. Analysis on distribution law, types and characteristics and development tendency of secondary geo-hazards induced by Lushan earthquake. *J. Eng. Geol.* **22**(02), 272–279. https://doi.org/10.13544/j.cnki.jeg.2014.02.014 (2014).
104. Pei, X. & Huang, R. Analysis of characteristics of geological hazards by 4·20 Lushan earthquake in sichuan, China. *J. Chengdu Univ. Technol. (Science Technol. Edition)*. **40** (03), 257–263 (2013).
105. Yin, Z., Zhao, W., Chu, H. & Sun, W. Basic characteristics of geohazards induced by Lushan earthquake and compare to them of Wenchuan earthquake. *Acta Geol. Sin.* **88**(06), 1145–1156 (2014).
106. Guo, Z., Tong, L., Zheng, X., Qi, J. & Wang, J. Remote sensing survey of secondary geological disasters triggered by Lushan earthquake in Sichuan Province and tentative discussion on disaster characteristics. *Remote Sens. Land. Resour.* **26**(03), 99–105 (2014).
107. Xu, C. et al. Landslides triggered by the aprial 20, 2013 lushan, Sichuan Province Ms7.0 strong earthquake of China. *Seismology Geol.* **35**(03), 641–660 (2013).
108. Xu, C., Xu, X., Zheng, W., Min, W. & Ren, Z. Landslides triggered by the 2013Minxian-Zhangxian, Gansu Province ms6.6 earthquake and its tectonic analysis. *Seismology Geol.* **35**(03), 616–626 (2013).
109. Xu, C., Xu, X. & Zheng, W. Compiling inventory of landslides triggered by Minxian-Zhangxian earthquake of July 22, 2013 and their Spatial distribution analysis. *J. Eng. Geol.* **21** (05), 736–749 (2013).
110. Tian, Y., Xu, C., Xu, X. & Chen, J. Analysis of parameters of landslides triggered by the Minxian-Zhangxian Ms6.6 earthquake. *China Earthq. Eng. J.* **35**(04), 761–767 (2013).
111. Tao, Y., Hu, K., Tian, Y., Ge, Y. & Chen, X. Distribution and characteristics of secondary mountain hazards triggered by Ludian earthquake in Yunnan. *J. Earth Sci. Environ.* **37**(04), 84–93 (2015).
112. Tian, Y. et al. Spatial distribution analysis of coseismic and per-earthquake landslides triggered by the 2014 Ludian Ms6.5 earthquake. *Seismology Geol.* **37**(01), 291–306 (2015).
113. Wang, Y., Yang, Y., Yan, X., Tang, P. & Zhang, J. Characteristics and causes of superhuge secondary geological hazards induced by M6.5 Ludian earthquake in Yunnan. *J. Catastrophology* **31**(01), 83–86 (2016).

114. Tang, Y., Che, A., Cao, Y. & Zhang, F. Risk assessment of seismic landslides based on analysis of historical earthquake disaster characteristics. *Bull. Eng. Geol. Environ.* **79**(5), 2271–2284 (2020).
115. Bai, X. et al. Modeling and testing earthquake-induced landslide casualty rate based on a grid in a Kilometer scale: taking the 2014 Yunnan Ludian Ms6.5 earthquake as a case. *J. Seismol. Res.* **44**(1), 87–95 (2021).
116. Dai, L. et al. A preliminary study on Spatial distribution patterns of landslides triggered by Jiuzhaigou earthquake in Sichuan on August 8th, 2017 and their susceptibility assessment. *J. Eng. Geol.* **25**(04), 1151–1164. https://doi.org/10.13544/j.cnki.jeg.2017.04.030 (2017).
117. Liu, G., Zhang, Y., Zhang, S., Ye, X. & Yuan, Y. Analysis on distribution characteristics of characteristics of secondary geo-hazards before and after Jiuzhaigou earthquake. *J. Geol. Hazards Environ. Preservation* **29**(03), 1–4 (2018).

Author contributions

Xia Chaoxu completed the writing of the manuscript, data processing, model construction, and other related tasks.Qi Wenhua has completed the writing and review of the introduction section of the manuscript.Li Huayue completed the data collection, processing, and model construction work.Nie Gaozhong's work on the ideas, overall structure, and other aspects of the manuscript.

Funding

This work was jointly supported by the National Natural Science Foundation of China (Grant No. 42207532) and the National Natural Science Foundation of China (Grant No. 42177453) and National Nonprofit Fundamental Research Grant of China, Institute of Geology, China Earthquake Administration (Grant No. IGCEA 1905), and the National Natural Science Foundation of China (Grant No. 41907397).

Declarations

Competing interests

The authors declare no competing interests.

Additional information

Correspondence and requests for materials should be addressed to X.C. or Q.W.